

THE EFFECTS OF GAMMA-RAY RADIATION
ON THE ELECTRICAL PROPERTIES
OF ZnSe SINGLE CRYSTAL

A THESIS

presented to

The Faculty of Graduate Studies

The University of Manitoba

In Partial Fulfillment

of the Requirements for the Degree

Master of Science in Electrical Engineering

by

Anthony Ka-Chung Ho

April, 1970



ACKNOWLEDGEMENT

The author sincerely expresses his gratitude for the guidance given by Dr. K.C. Kao under whose direction this thesis was conceived. Also, he wishes to thank Mr. R. Woods for assistance in the construction of experimental apparatus, and Mrs. S.B. Ryan for typing this thesis.

Finally, he wishes to acknowledge his indebtedness to the National Research Council of Canada for the financial support under Grant A-3339.

TABLE OF CONTENTS

	PAGE
LIST OF FIGURES	v
LIST OF TABLES	viii
ABSTRACT	ix
CHAPTER I INTRODUCTION	1
CHAPTER II LITERATURE REVIEW ON II-VI COMPOUND SEMICONDUCTORS	4
2.1 Some Important Factors Determining the Electrical Properties	4
2.1.1 Point Defects	4
2.1.2 Carrier Lifetime and Mobilities	6
2.1.3 Scattering Mechanisms	11
2.2 Electrical Properties	14
2.2.1 Cadmium Sulfide	14
2.2.2 Cadmium Selenide	20
2.2.3 Zinc Selenide	20
2.2.4 Zinc Telluride	23
2.3 The Effects of Radiation	25
2.3.1 The Effects of Irradiation with Gamma Rays in II-VI Compound Semiconductors	25
2.3.2 Fluorescence in CdS	34
2.3.3 Fast Neutron Irradiation Effects in CdS	38
2.3.4 The Change of Electrical Properties by Thermal Treatment in ZnSe	40

	PAGE
2.3.5 Threshold Energies for Electron Radiation Damage in ZnSe	42
2.3.6 Photoelectronic Evaluation of Electron Radiation Damage in CdS	46
CHAPTER III THEORY OF RADIATION EFFECTS	47
CHAPTER IV EXPERIMENTAL METHODS AND RESULTS	57
4.1 Experimental Apparatus and Procedures	57
4.2 Experimental Results	64
CHAPTER V ANALYSIS AND DISCUSSION OF EXPERIMENTAL RESULTS	75
CHAPTER VI CONCLUSION	85
BIBLIOGRAPHY	87

LIST OF FIGURES

FIGURE		PAGE
2.1	The Temperature Dependence of the Hall Mobility in Undoped n-type CdS	17
2.2	Electrical Conductivity as a Function of Temperature for CdS Single Crystal	18
2.3	Hall Coefficient as a Function of Temperature for CdS Crystals	18
2.4	The Temperature Dependence of Hall Mobility of CdS Crystals	19
2.5	The Temperature Dependence of the Hall Mobility of Several n-type CdSe Crystals	21
2.6	The Temperature Dependence of the Hall Mobility of n-type ZnSe Crystals	22
2.7	The Temperature Dependence of the Hall Mobility of Undoped and Ag Doped p-type ZnTe Crystals	24
2.8	Gamma Irradiation Characteristics at Room Temperature	27
2.9	CdS Irradiated with Various Doses ^{60}Co Gamma Rays	29
2.10	CdS Irradiated with ^{137}Cs Gamma Rays	30
2.11	CdTe Irradiated with ^{60}Co Gamma Rays	31
2.12	CdTe Irradiated with ^{137}Cs Gamma Rays	31
2.13	CdS Irradiated with Thermal Neutrons	32
2.14	Spectra of CdS at 80°K Before and After Electron Bombardment at 500KeV	36
2.15	Temperature Dependence of Hall Mobility and Hall Coefficient for a Cd Doped ZnSe Crystal Fired in Liquid Zn	41
2.16	Spectra of ZnSe at 80°K Before and After Electron Bombardment at 500KeV	43
2.17	Rate of Increase in Fluorescence at 80°K in ZnSe as a Function of Electron Energy	43

FIGURE		PAGE
2.18	The Spectra of ZnSe at 10°K Before and After Electron Bombardment at 350KeV	45
2.19	The Rate of Radiation Damage in ZnSe vs Electron Bombardment Energy	45
3.1	Compton Absorption Coefficient per Electron as a Function of Energy	50
3.2	Diagram Showing the Photon Energy and the Crystal Atomic Number Z at which the Principal Gamma-Quantum Absorption Process Becomes Dominant	52
4.1	Circuit Arrangement for Hall Effect and Conductivity Measurements	58
4.2	Apparatus for Hall Measurements for Temperatures Down to 77°K	59
4.3	Sample Holder for Measurements	60
4.4	Geometry and Dimensions of ZnSe Crystal Sample	62
4.5	The Voltage Dependence of Dark Current in ZnSe Crystal Before Irradiation	65
4.6	The Voltage Dependence of Dark Current Before and After Irradiation with Gamma Rays	66
4.7	The Temperature Dependence of Resistivity in ZnSe Before and After Irradiation with Gamma Rays (Applied Voltage 50V)	68
4.8	The Temperature Dependence of Resistivity in ZnSe Before and After Irradiation with Gamma Rays (Applied Voltage 200V)	69
4.9	The Temperature Dependence of Resistivity in ZnSe Before and After Irradiation with Gamma Rays (Applied Voltage 400V)	70
4.10	Dependence of Resistivity of ZnSe Crystal on Radiation Dosage	71

FIGURE		PAGE
4.11	The Temperature Dependence of Hall Mobility Before and After Irradiation with Gamma Rays	72
4.12	The Effect of Gamma Irradiation on the Hall Mobility in ZnSe Crystal	73
4.13	The Temperature Dependence of Hall Coefficient Before and After Irradiation with Gamma Rays	74
5.1	Comparison of the Experimental Results of the Hall Mobility Before Gamma Irradiation with Theory	84

LIST OF TABLES

TABLES	PAGE
2.1 Theoretical Mobilities of Carriers in II-VI Compound Semiconductors at 300°K	16
2.2 Physical Properties of II-VI Compound Semiconductors at 300°K	26

ABSTRACT

The effects of gamma radiation on the dark resistivity and Hall mobility in high purity ZnSe single crystals have been investigated at various temperatures. The gamma irradiation is conducted in a cobalt 60 gamma cell with an average dose rate of 1.2×10^6 rads/hr. Following radiation, the dark current decreases as the radiation dose increases. The resistivity of ZnSe crystal changes from $\sim 10^8$ ohm-cm to $\sim 10^{10}$ ohm-cm at room temperature. The Hall mobility decreases from ~ 500 cm²/V-sec to a limiting value of ~ 170 cm²/V-sec. Before radiation, a single donor ionization energy $E_D = 0.316$ eV below the conduction band edge is obtained from the result of the temperature dependence of the Hall coefficient. The corresponding concentration of donors and compensating acceptors are respectively $N_D = 1.19 \times 10^{11}$ cm⁻³ and $N_A = 3.94 \times 10^{10}$ cm⁻³. After gamma irradiation, the donor ionization energy level changes to 0.377 eV below the conduction band. The values of N_D and N_A in this level are 1.17×10^9 cm⁻³ and 3.71×10^8 cm⁻³ respectively. The results indicate that irradiation with gamma rays leads to predominantly acceptor type defects in ZnSe and the predominant scattering mechanism limiting the lattice mobilities is the polar interaction with the longitudinal optical phonons.

CHAPTER I

INTRODUCTION

The first research papers on II-VI compounds dated back to the middle of the Nineteenth Century. The early work was carried out on pressed, powdered or sintered specimens, which often led to confusing and conflicting results. Until a decade ago, successful growth of single crystals of II-VI compounds in high purity form has made it possible to apply new research techniques to old problems and to attack new ones. It is now possible to achieve very high photosensitivities in all II-VI compounds; the range of band gaps in II-VI compounds covers a range of maximum photosensitivities from the near ultraviolet to the near infrared. The successful application of scattering theory to the study of transport properties of n-type II-VI compounds has laid a solid foundation to the understanding of the electrical properties of these materials. Since the technology of single crystal growth has been extensively developed, actual or potential opportunities for commercial application have multiplied. From a materials research viewpoint, II-VI compounds combine all the challenges and fascinations of the more ionic I-VII insulators and the more covalent III-V semiconductors.

The purpose of investigating radiation effects in solids is twofold: first to use the radiation as a tool to study the properties of solids and second to study the radiation damage in solids under various radiation environments. Fast particle bombardment provides a means of controlled introduction of lattice defects into crystalline solids and hence is an

excellent method for studying in a general way the influence of lattice defects on the physical properties of solids. From an application point of view, it is important to investigate the behaviour of semiconductors which form part of solid state devices, under various radiation environments with a view to developing a better understanding of the mechanisms responsible for causing any change of electronic properties of such materials and a new approach to the design of solid state devices for use in radiation environments. Furthermore, a study of defect stability is extremely important from the practical point of view. It is obvious that if defects could give rise to new and desirable properties in a semiconductor, it is desirable to retain these properties throughout the service life of a device made from this semiconductor.

Many investigations have studied the effects of radiation in single elements in the past twenty years. However, the full interpretation of the radiation effects on II-VI compound semiconductors is still not available.

Although a much larger group of compounds could be referred to as II-VI compounds, the present work is confined specifically to the ZnSe (Zinc Selenide) because ZnSe is one of the II-VI compounds which has not been well investigated up-to-date. The effect of irradiation with 1.2×10^6 rads/hr. ^{60}Co gamma rays on the electrical properties in ZnSe has been studied by means of conductivity and Hall mobility measurements at various temperatures and fields. In this thesis, Chapter II gives a brief review of the previous

works on the general properties of some II-VI compound semiconductors.

The theory of radiation effects is described in Chapter III, and the experimental methods and results in Chapter IV. Analysis and discussion of results are given in Chapter V and conclusions in the final Chapter.

CHAPTER II

LITERATURE REVIEW ON II-VI COMPOUND SEMICONDUCTORS

2.1 Some Important Factors Determining the Electrical Properties

2.1.1 Point Defects

The deviation from hypothetical perfect crystal structure can be described in terms of defects. Comparing with line defects and plane defects, the point defects of various types are more important in determining the electrical properties of II-VI compounds. In point defects, it can be classified into native point defects and the foreign (or impurity) point defects. For example, the native point defects are misplaced lattice atoms (or ions), interstitials, vacant lattice sites, and zero-dimensional associates between them, and electrons and holes. The isolated native point defects appear to be very unstable at room temperature, and they either tend to associate themselves with other defects, or precipitate out during the cooling of the sample.

The effect of those imperfections is to introduce discrete energy levels in addition to the levels for the perfect crystal, provided they are far enough apart to be treated as isolated centres of potential in the crystal. When there is a high density of impurity centres, the level will interact and may form sub-bands (impurity bands). Such sub-bands have a marked effect on the conductivity of certain semiconductors at low temperatures.

The binding energy ' ϵ_1 ' of the electrons and ' ϵ_2 ' of the holes, to the impurity centre, are given by

$$\epsilon_1 = m_e^* E_H / n_i^2 K^2 m \quad (2.1)$$

$$\epsilon_2 = m_h^* E_H / n_i^2 K^2 m \quad (2.2)$$

where ' E_H ' is the ionization energy of the ground state of the hydrogen atom ($\approx 13.6\text{eV}$), ' n_i ' is an integer, ' m_e^* ' is the effective mass of electrons in the conduction band, ' m_h^* ' is the effective mass of holes in the valence band, ' K ' is the static dielectric constant of the semiconductor, and ' m ' is the mass of an electron in free space.

Besides, the effective radius ' α ' of the impurity centre when occupied by an electron in the ground state is given by

$$\alpha = \frac{m}{m_e^*} K a_0 \quad (2.3)$$

where ' a_0 ' is the Bohr radius which is $0.53 \times 10^{-8}\text{cm}$. In II-VI compounds, the effective masses are generally larger and dielectric constants smaller than those of the element semiconductors such as Ge and Si. Hence, the electrons are more tightly bound, the wave function does not spread as much and central cell corrections are more important in II-VI compounds than in

Ge and Si semiconductors.

Experimentally, De Nobel (1959) proposed that a donor level of 0.02eV below the conduction band edge of CdTe was due to interstitial Cd, and Lorenz (1964) showed that the n-type conductivity observed in the high purity CdTe was due to residual impurities. Woodbury (1964) has suggested that the concentration of any electrically active interstitial Cd even in the purest CdS crystals available is always lower than the residual concentration of shallow foreign donors. Reynolds and Stevenson (1966) have suggested that interstitial Te may act as a double acceptor in ZnTe on the basis of self-diffusion measurement. The native defects in II-VI compounds have been investigated; most are the Zn and Cd vacancies. Also, it has been suggested that isolated cation vacancies may act as a double acceptor in ZnTe (Aven and Segall, 1963) and CdTe (Lorenz and Segall, 1963).

2.1.2 Carrier Lifetime and Mobilities

The band structure is another important factor determining the electrical properties of II-VI compounds. For example, the behaviour of the mobility depends upon the effective mass which is inversely proportional to the curvature of the band. Consider the effect of collision on the motion of the electrons and positive holes in semiconductors under the influence of electrical and magnetic fields. For a certain assumption, the average time ' \bar{t} ' between collision is given by

$$\bar{t} = \frac{1}{n_0} \int_0^\infty \frac{nt \, dt}{\tau} = \tau \quad (2.4)$$

where ' n_0 ' is the number of electrons moving in a certain direction at $t = 0$, ' τ ' is the so-called mean free time. Suppose that the electrons are moving in the crystal under an applied electric field \bar{E} which is in x-direction. Its x-component of velocity, ' \bar{v}_x ' can be written as

$$\bar{v}_x = \bar{v}_{x0} - \frac{\bar{E}q\tau}{m_e^*} \quad (2.5)$$

where ' \bar{v}_{x0} ' is the velocity of electrons in the x-direction at $t = 0$, ' q ' is the electronic charge. Assuming $v_{x0} = 0$, we have

$$\bar{v}_x = - \frac{q\bar{E}\tau}{m_e^*} = - \mu_e \bar{E} \quad (2.6)$$

where ' μ_e ' is the electron mobility defined by

$$\mu_e = q\tau/m_e^* \quad (2.7)$$

Similarly, for positive holes,

$$\bar{v}_x' = q\tau'\bar{E}/m_h^* \quad (2.8)$$

The hole mobility is given by

$$\mu_h = q\tau'/m_h^* \quad (2.9)$$

where ' τ ' is the mean free time for the holes. If there are ' n ' electrons in the conduction band and ' p ' holes in the valence band, the current density in the x -direction can be written as

$$\bar{J}_x = q(n\mu_e + p\mu_h)\bar{E} \quad (2.10)$$

and the conductivity is given by

$$\sigma = q(n\mu_e + p\mu_h) \quad (2.11)$$

For simplicity, the mean free time ' τ ' has been regarded as being the same for all electrons. In fact, ' τ ' depends on the velocity of the electron or hole being scattered, and may also depend on the direction of motion through the crystal. Generally, some correct weighing function which determines the average relaxation time $\langle\tau\rangle$ can be found. However, the drift velocity and mobility of electrons is more conveniently written in terms of $\langle\tau\rangle$ as

$$\bar{v}_x = q\bar{E}\langle\tau_e\rangle/m_e^* \quad (2.12)$$

and

$$\mu_e = q\langle\tau_e\rangle/m_e^* \quad (2.13)$$

When a magnetic field is applied to the crystal carrying a current in a direction at right angles to the current, an e.m.f. is produced across the crystal in a direction perpendicular to the current and to the magnetic field. This effect is well known as the Hall effect and it is one of the most powerful tools for studying the electronic properties of semiconductors.

The Hall coefficient for n- and p-type non-degenerate semiconductors is given by

$$R_H = - \frac{r_H}{nq} = - \frac{1}{nq} \frac{\langle \tau_e^2 \rangle}{\langle \tau_e \rangle^2} \quad (2.14)$$

and

$$R_H = \frac{r_H'}{pq} = \frac{1}{pq} \frac{\langle \tau_h^2 \rangle}{\langle \tau_h \rangle^2} \quad (2.15)$$

For mixed conductors, it can be shown that

$$R_H = - \frac{1}{q} \frac{r_H b^2 n - r_H' n}{(bn+p)^2} \quad (2.16)$$

where b is the mobility ratio μ_e/μ_h . The Hall factor is defined by

$$r_H \equiv nqR_H \equiv \frac{\mu_H}{\mu} \quad (2.17)$$

where 'n' is the carrier concentration, ' μ_H ' is the Hall mobility and ' μ ' is the drift mobility.

The relation of the motion of electrons and the external field of force can be written as

$$m_e^* \frac{d\bar{v}}{dt} = \bar{F} \quad (2.18)$$

where the velocity vector ' \bar{v} ' is given by

$$\bar{v} = \hbar^{-1} \nabla_K E(K) \quad (2.19)$$

When an electric field and a magnetic field are simultaneously applied to the semiconductor, \bar{F} is given by

$$\bar{F} = -q\bar{E} - q(\bar{v} \times \bar{B}) \quad (2.20)$$

where \bar{B} is the magnetic flux density. In general, the effective mass of the hole will not be the same as that of an electron since they arise from different bands. For the spherically symmetrical case, the effective mass tensor can be written as

$$\frac{1}{(m_e^*)_{ij}} = \hbar^{-2} \frac{\delta^2 E_c}{\delta k_i \delta k_j} \quad (2.21)$$

and

$$\frac{1}{(m_h^*)_{ij}} = -\hbar^{-2} \frac{\delta^2 E_v}{\delta k_i \delta k_j} \quad (2.22)$$

It can be noted that ' m_e^* ' and ' m_h^* ' are inversely proportional to the curvature of the constant energy surface in k-space.

In the presence of a magnetic field, the resistance depends upon the magnetic field, and it may be shown that the low field transverse magnetoresistance $\Delta\rho/\rho$ may be conveniently measured by a parameter ' ξ ' defined by

$$\xi \equiv \Delta\rho/\rho (\mu_H)^2 \quad (2.23)$$

This parameter is independent of the magnitude of the scattering and depends only on its energy dependence.

2.1.3 Scattering Mechanisms

The electrical properties of II-VI compounds depend also upon a combination of several scattering processes such as piezoelectric and polar optical mode scattering.

Most conventional scattering mechanisms can be described by a relaxation time $\langle \tau \rangle$ or mobility ' μ '. The theory of polar optical mode scattering has been reviewed by Frölich (1954) who showed that a perturbation theory is applicable for values of ' α ' [a coupling constant of the high frequency (or bare) mass and the low frequency (or polaron) mass] small compared with unity. The expression for mobility given by Frölich is

$$\mu_o = (16.91/z^{1/2}) \left(\frac{1}{n_r^2} - \frac{1}{K} \right)^{-1} \left(\frac{m}{m^*} \right)^{3/2} (e^{-z/T} - 1) \quad (2.24)$$

where ' n_r ' is the optical index of refraction and ' z ' ($=\hbar\omega/kT$) is the characteristic temperature and ' ω ' is the angular frequency of longitudinal optical phonons, ' m^* ' is the effective mass of electrons (or holes). The piezoelectric scattering can occur in a crystal which has a piezoelectric effect and it is due to the electric fields produced by acoustic phonons. Blatt (1957) has derived the expression for the piezoelectric mobility, and it is

$$\mu_p = \left(\frac{16}{3} \sqrt{2\pi} \right) \left\{ \hbar^2/qm^*{}^{3/2} (kT)^{1/2} \right\} \left\{ \sum_{\text{modes}} \frac{\langle \kappa^2 \rangle}{K\epsilon_o} \right\}^{-1} \quad (2.25)$$

where ' κ^2 ' is a suitable average of the piezoelectric electrochemical coupling constant, ' K ' is the static dielectric constant. Then, the

mobility due to the lattice scattering can be written as

$$\frac{1}{\mu_{\text{lattice scattering}}} = \frac{1}{\mu_o} + \frac{1}{\mu_p} \quad (2.26)$$

The mobility measured at 77°K is considerably lower than the value predicted theoretically for pure lattice scattering. The discrepancy is probably due to ionized impurity scattering which is important in impure and non-stoichiometric compounds. The expression for mobility due to ionized impurity scattering given by Brooks (1955) is

$$\mu_i = \frac{4(2/\pi)^{3/2}(kT)^{3/2}(4\pi \epsilon_o K)^2}{q^3 m^{*1/2} N_I [\ln(b) - 1]} \quad (2.27)$$

where

$$b = \frac{6m^*(kT)^2 (4\pi \epsilon_o K)}{\pi q^2 \hbar^2 n'} \quad (2.28)$$

in thermal equilibrium,

$$n' = n + (N_D - N_A - n)(n + N_A)/N_D \quad (2.29)$$

and

$$N_I = n + 2N_A \quad (2.30)$$

where 'n' is the carrier concentration, ' N_A ' is the acceptor concentration, and ' N_D ' is the concentration of the donors.

The theoretical mobilities of carriers in II-VI compound semiconductors at 300°K. are given in Table 2.1.

2.2 Electrical Properties

2.2.1 Cadmium Sulfide

Since the band gap in CdS which is 2.24eV at 300°K is quite large, the intrinsic carrier concentration is very low and the carrier concentration is therefore mainly determined by impurities or native defects. The effective mass has been obtained by a number of investigators with impurity concentration, binding energy and dielectric constants taken into account. Zook (1963) measured m_e^*/m to be 0.19 which is in good agreement with the theory. Devlin (1965) reported that $m_e^*/m = 0.20$ is the most reliable value when the effects of piezoelectric scattering and optical mode scattering on the Hall mobility are considered, and the temperature dependence of the static dielectric constant is taken into account. The temperature dependence of the Hall mobility in undoped n-type

CdS given by Devlin is shown in Fig. 2.1.

The energy bands are expected to be anisotropic at $K = 0$ due to the hexagonal structure of the CdS crystal. There have been several measurements of the anisotropy of the conductivity and the mobility. Masumi (1959) measured the conductivity anisotropy as a function of temperature. A similar result has also been reported on the anisotropy of the mobility by Zook and Dexter (1963). They concluded that the anisotropy of the magneto-resistance is consistent with a single anisotropy valley at $K = 0$.

Spear and Mort (1963) obtained the same values for the hole mobility of all their samples but the electron mobilities were considerably different from sample to sample.

In Figs. 2.2 and 2.3 are given some typical experimental results on the temperature dependence of conductivity and Hall coefficient in CdS obtained by Itakura and Toyoda (1963). The Hall mobilities ' μ_H ' calculated from 'R', also shown in Fig. 2.4 from which the activation energy ΔE is calculated to be 0.014eV for the temperature range from 200°K to 50°K, and 0.007eV from 50°K to 10°K. They interpreted these results as being due to two kinds of donor levels, one with a concentration of $1.5 \times 10^{17} \text{cm}^{-3}$ at 0.014eV and the other with more than 10^{16}cm^{-2} at 0.007eV below the conduction band. It can be seen from Fig. 2.4 that the Hall mobility is

TABLE 2.1

*Theoretical Mobilities of Carriers (in cm²/V-sec) in II-VI Compound
Semiconductors at 300°K [after Devlin (1965)]*

	<i>CdS</i>	<i>CdSe</i>	<i>CdTe</i>	<i>ZnS</i>	<i>ZnSe</i>	<i>ZnTe</i>
$\mu_e(\text{opt. mode})$	330	630	1320	344	600	-
$\mu_h(\text{opt. mode})$	38.5	98	190	-	90	114
$\mu_e(\text{piezo.})$	4360	1.5×10^4	1.5×10^6	-	3.7×10^5	-
$\mu_h(\text{piezo.})$	406	1.23×10^3	2.1×10^5	-	5.5×10^4	1.5×10^5

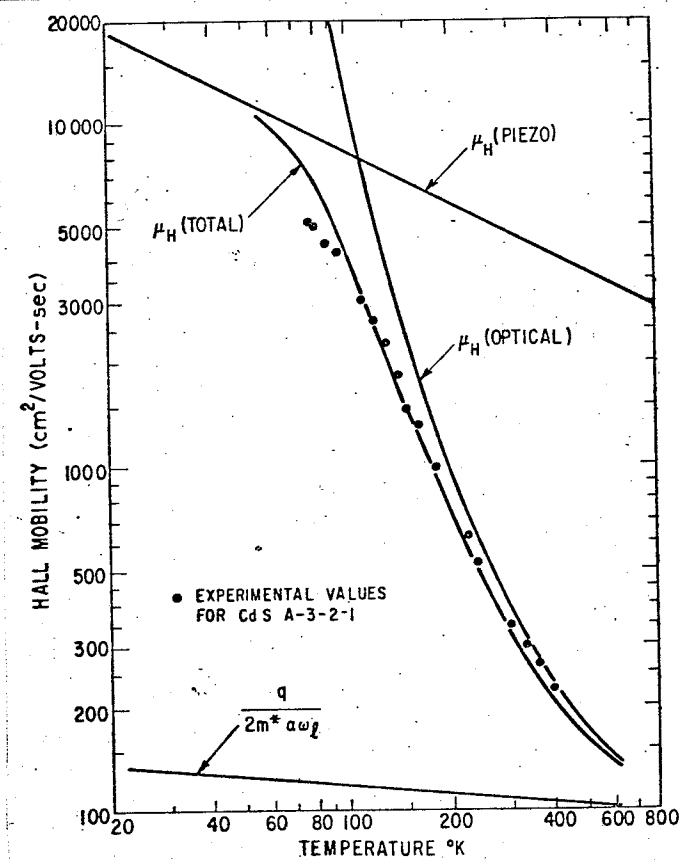


Fig. 2.1

The temperature dependence of the Hall mobility in undoped n-type CdS. The solid curve is the theoretical intrinsic Hall mobility due to piezoelectric and optical mode scattering assuming $m_e^*/m_e = 0.20$. The line at the bottom indicates the temperature dependence where μ_F is Fröhlich's (1954) low temperature approximation for the mobility and $Z = \hbar\omega_e/KT$, and α is the polaron coupling constant.

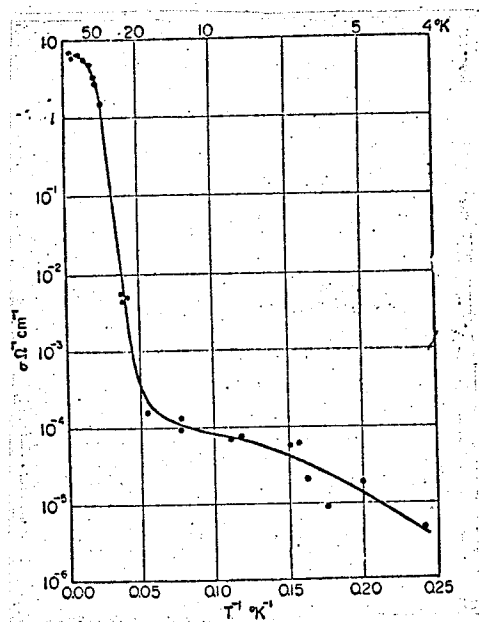


Fig. 2.2

Electrical conductivity as a function of temperature for CdS (Itakura & Toyoda, 1963)

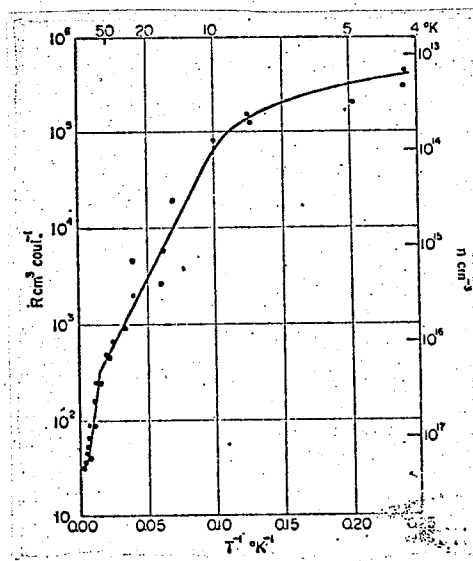


Fig. 2.3

Hall coefficient as a function of temperature for CdS (Itakura & Toyoda, 1963)

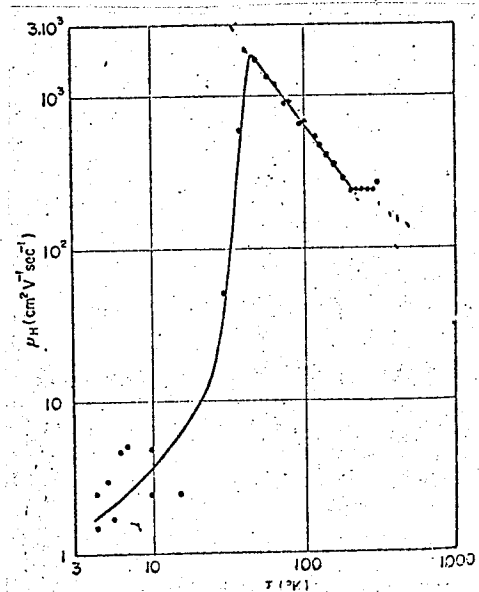


Fig. 2.4

Temperature dependence of Hall mobility of CdS crystals (Itakura & Toyoda, 1963)

constant and equal to about $200\text{cm}^2/\text{V-sec}$ from 300°K to 200°K , and

$\mu_H = 6.4 \times 10^4 T^{-3/2}$ from 200°K to 50°K . They suggested that the relation $\mu_H \propto T^{-3/2}$ may be due to the acoustical phonon scattering of carriers. Below 50°K , the Hall mobility decreases quite rapidly and falls down to about $1\text{cm}^2\text{V}^{-1}\text{sec}^{-1}$ at liquid helium temperature.

2.2.2 Cadmium Selenide

The electrical properties of CdSe are very similar to those of CdS but it has a smaller electron effective mass, larger mobility and smaller piezoelectric coupling. The effective mass has been measured by Wheeler and Dimmock (1962) to be $m^* = 0.13m$ and it has been found that this value is in good agreement with the theoretically predicted value. Devlin (1965) has calculated the combined effects of the optical mode scattering and piezoelectric scattering and obtained the Hall mobilities for several samples. They are shown in Fig. 2.5.

2.2.3 Zinc Selenide

The temperature dependence of the Hall mobility of electrons in ZnSe obtained by Aven and Kennicott (1964) is shown in Fig. 2.6. Aven and Segall (1963) found that the optical mode scattering is the only significant intrinsic scattering mechanism, the impurity scattering becomes significant only at low temperatures.

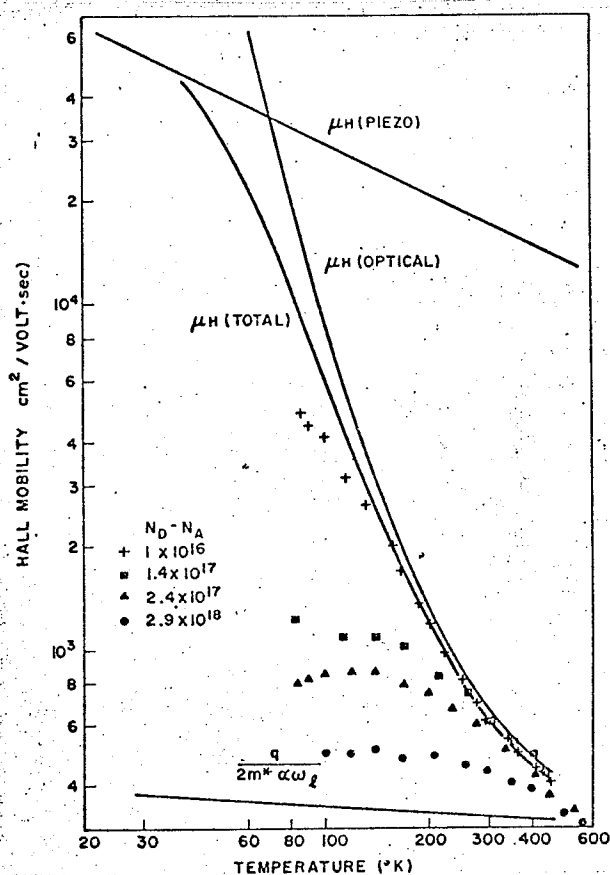


Fig. 2.5

The temperature dependence of the Hall mobility of several n-type CdSe crystals. The three lower samples were doped with Ga while the fourth was undoped. The solid line indicates the theoretical Hall mobility due to the combined effect of piezoelectric and optical mode scattering treated variationally using $m^*/m = 0.13$. The line at the bottom indicates the temperature dependence of $\mu_F/(e^Z - 1)$ (where μ_F is Fröhlich's (1954) low temperature approximation for the mobility and $Z = \hbar\omega_e/kT$, and α is the polaron coupling constant) i.e. the temperature dependence of the material constants specifically, the static dielectric constant.

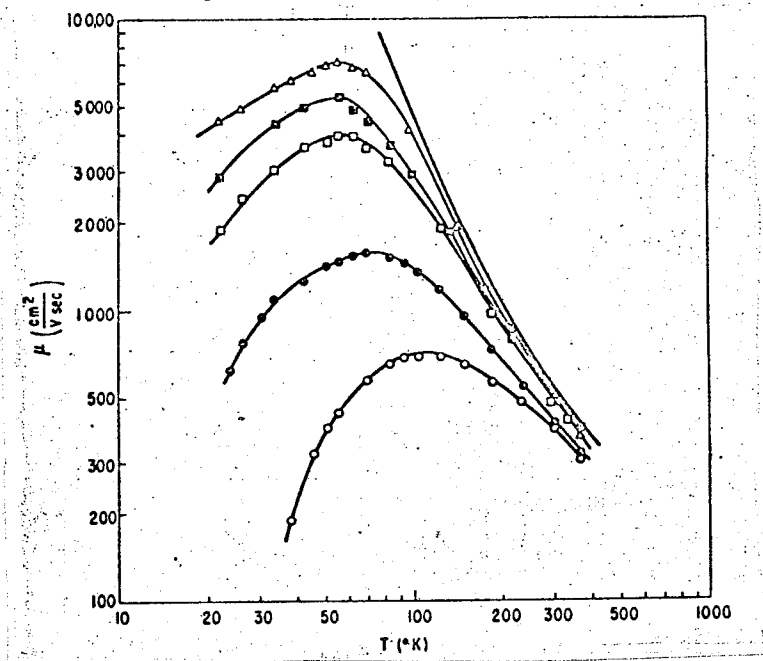


Fig. 2.6

The temperature dependence of the Hall mobility of n-type ZnSe crystals. The donor and acceptor concentrations in units of 10^{16} cm^{-3} are: triangles $N_D = 0.34$, $N_A = 0.13$; full squares $N_D = 1.8$, $N_A = 0.5$; open squares $N_D = 1.05$, $N_A = 0.75$; full circles $N_D = 3.7$, $N_A = 0.5$; open circles $N_D = 7.4$, $N_A = 3.4$. The solid line is the calculated drift mobility, taking into account the temperature dependence of the static dielectric constant, and using the electron effective mass of $0.17m$. (Aven and Kennicott, 1964)

The effective mass of ZnSe has been obtained by fitting the observed mobility to the theory of optical mode scattering given by Aven and Segall (1963). Marple (1964) found that the electron effective mass deduced from infrared Faraday rotation and reflectance measurements turns out to be 0.17m.

2.2.4 Zinc Telluride

The band gap energy determined optically at room temperature for Zn is 2.26eV which is comparatively smaller than that for ZnS (~3.6eV) and ZnSe (~2.7eV). The temperature dependence of Hall mobility of holes in ZnTe which were obtained by Aven and Segall (1963) is shown in Fig. 2.7.

It is interesting to note that the properties of semiconductors can be roughly predicted from the following trends: (Putley, 1960)

- (1) As the atomic weight increases, the energy gap becomes successively smaller.
- (2) The energy gaps tend to become smaller as the degree of ionic binding decreases and the degree of covalent bonding increases.
- (3) The mobility of materials containing heavier elements tends to be greater than those containing lighter elements.

These trends hold true for II-VI compound semiconductors.

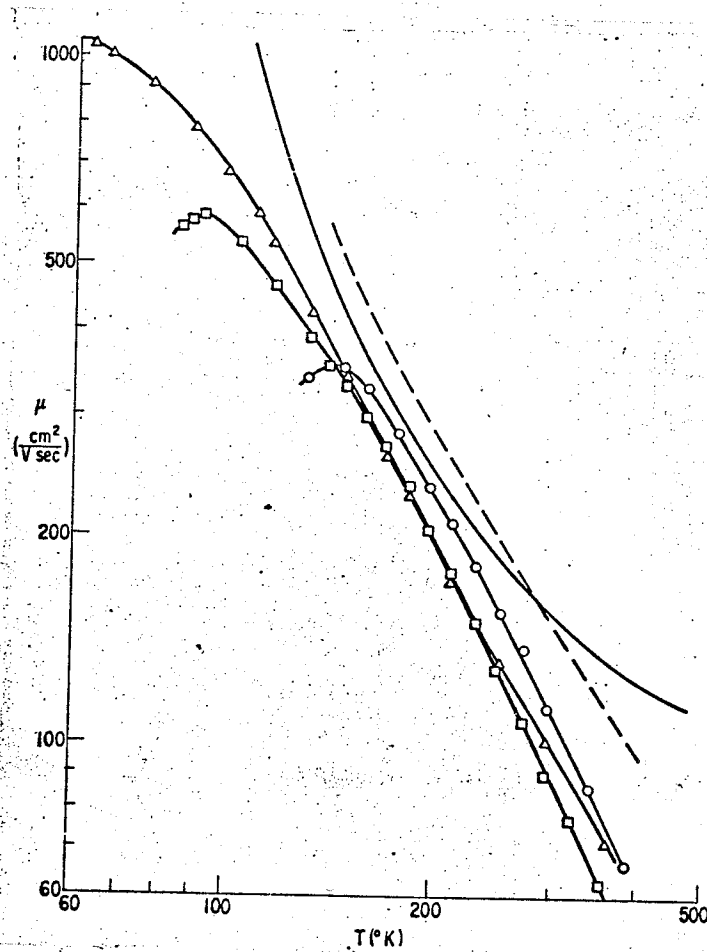


Fig. 2.7

The temperature dependence of the Hall mobility of two undoped (circles and squares) and Ag doped (triangles) p-type ZnTe crystals. The solid curve is the mobility due to pure optical mode scattering while the dashed curve represents the effect of an assumed temperature dependence of the static dielectric constant. (Aven and Segall, 1963).

Some of the experimental results of mobilities and effective mass ratio of II-VI compounds at 300°K are given in Table 2.2.

2.3 The Effects of Radiation

2.3.1 The Effects of Irradiation with Gamma Rays in II-VI Compound Semiconductors

The variation in electric resistance on single crystals of CdS, CdSe, ZnS, ZnSe, and ZnTe due to irradiation with a gamma ray source ^{60}Co of 3000 Curie intensity have been measured by Ikawa, Matumura and Suzuki (1962). It has been observed that in the region of gamma rays from ^{60}Co (1.17 and 1.33MeV), the Compton collision is the predominant mode of interaction between radiation and matter. Their results are shown in Fig. 2.8.

Chester (1966) measured the Hall effect in CdS and CdTe after the samples have been irradiated with three types of radiation sources: a ^{60}Co source which provided an approximately uniform flux of 7×10^{15} gamma photons (1.17 and 1.33MeV)/sq.cm.h., a ^{137}Cs source which provided 4.4×10^{15} gamma photons (0.662MeV)/sq.cm.h., and thermal neutron which has a flux of 7.5×10^{11} neutrons/sq.cm.sec. at a reactor power of 1MW. The experimental results for CdS and CdTe samples before and after gamma ray irradiation are shown in Figs. 2.9, 2.10, 2.11, and 2.12, and those for thermal neutron irradiated CdS in Fig. 2.13.

TABLE 2.2

PHYSICAL PROPERTIES OF II-VI COMPOUND SEMICONDUCTORS AT 300°K
(after Aven and Prener, 1967)

PROPERTY	CdS	CdSe	CdTe	ZnS	ZnSe	ZnTe
E_g	2.41	1.670	1.44	3.6	2.7	2.26
m_e^*/m	0.204	0.13	0.096	0.27 C	0.17	-
$\mu_e(300^\circ K)$	350	650	1050	140	530	340**
$\mu_e(max)$	1.1×10^4	5000	6×10^4	300	7200	-
m_h^*/m	$\begin{smallmatrix} 5.0 C \\ 0.7 \perp C \end{smallmatrix}$	$\begin{smallmatrix} >1 C \\ 0.45 \perp C \end{smallmatrix}$	0.35	$0.58 \perp C$	0.6	0.6
$\mu_h(300^\circ K)$	15	-	80	5(700°K)	28	110
$\mu_h(max)$	20	-	500	-	-	2200

** observed under illumination

E_G in eV, mobilities in $cm^2/V\text{-sec}$

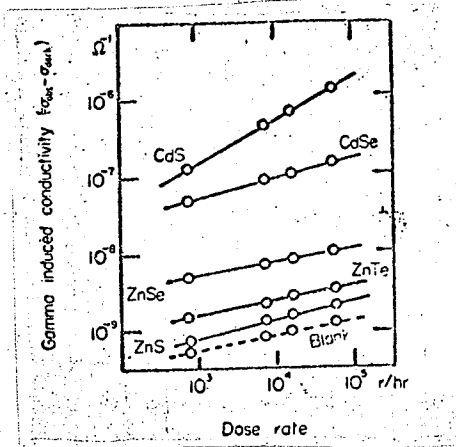


Fig. 2.8

Gamma irradiation characteristics at room temperature. Black; values observed without sample probably due to ionization current through the sample holder and the atmosphere. (Ikawa, Matsumura and Suzuki, 1962)

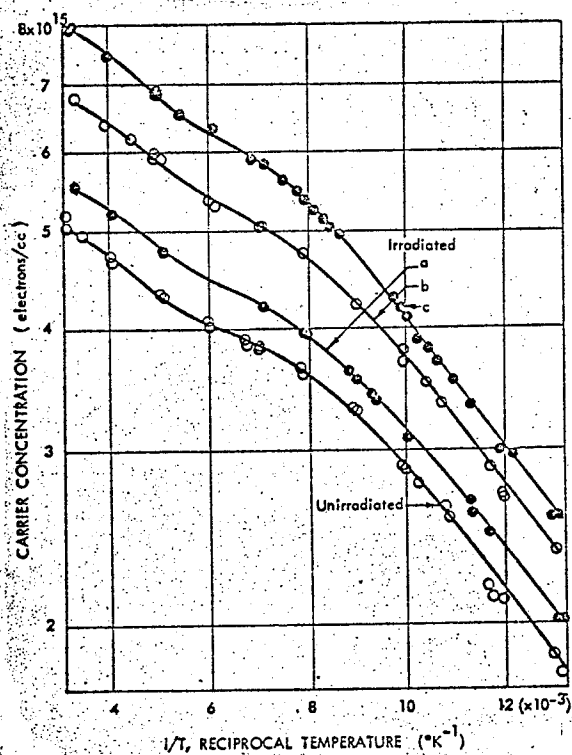


Fig. 2.9

Cadmium sulfide irradiated with various doses of ^{60}Co gamma rays.

(a) 1.8×10^{17} photons/cm²

(b) 1.14×10^{18}

(c) 2.25×10^{18}

(Chester, 1967)

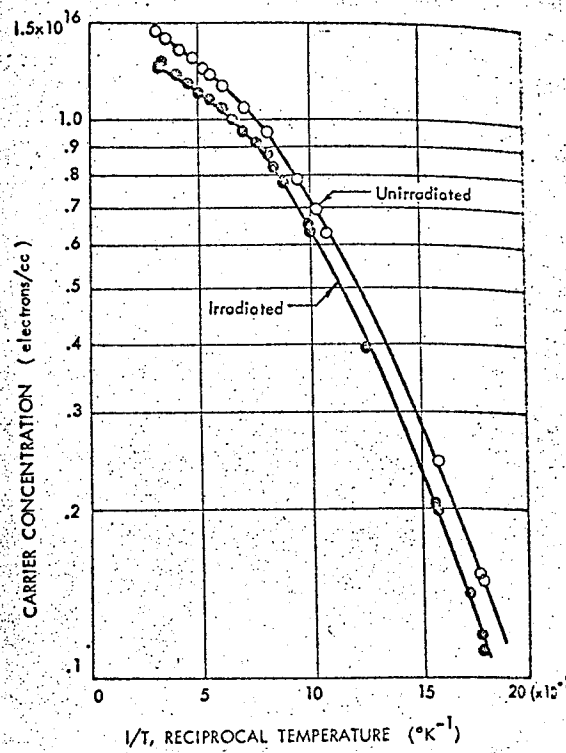


Fig. 2.10

Cadmium sulfide irradiated with 9.5×10^{17}
 ^{137}Cs gamma ray photons/cm².
 (Chester, 1967)

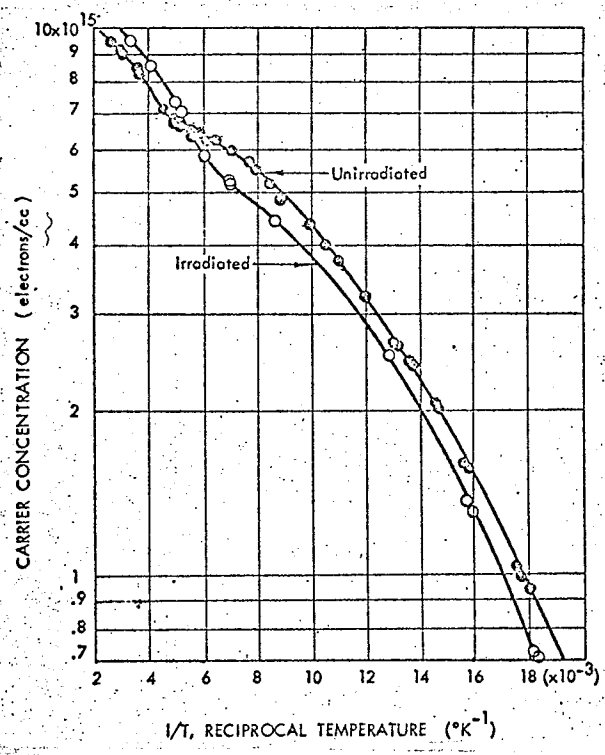


Fig. 2.11

Cadmium telluride irradiated with 1.4×10^{16} ⁶⁰Co gamma ray photons/cm². (Chester, 1967)

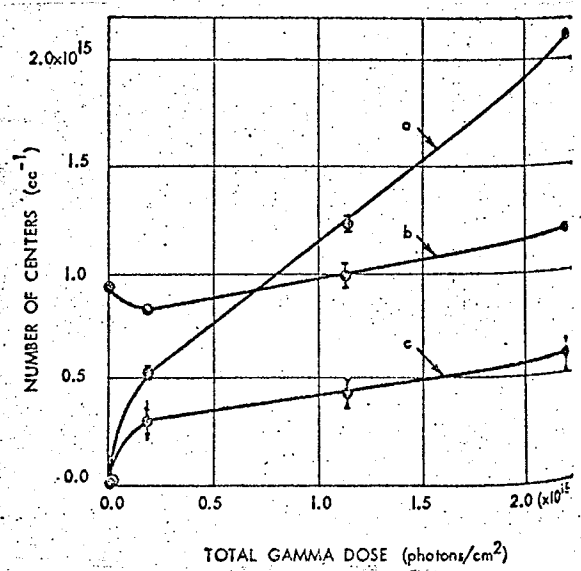


Fig. 2.12

Cadmium telluride irradiated with 8.8×10^{16} ¹³⁷Cs gamma ray photons/cm². (Chester, 1967)

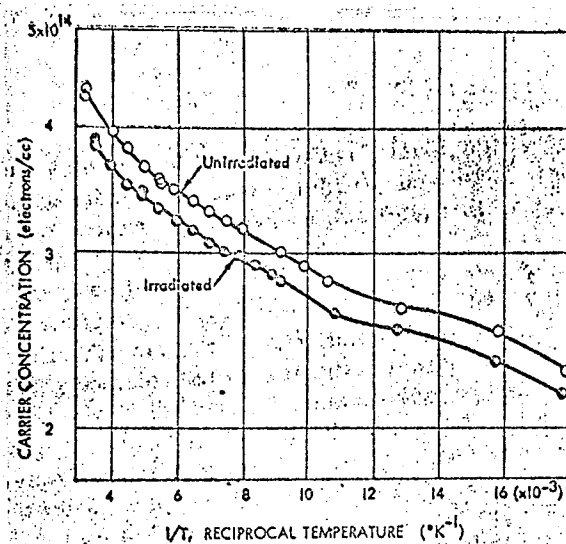


Fig. 2.13 Cadmium sulfide irradiated with 2.8×10^{12} thermal neutrons/cm². (Chester, 1967)

Chester found that irradiation of these materials at room temperature did not introduce any energy levels in the range from 0.02 to 0.2eV below the conduction band although the density of levels initially present in this interval was altered, and under certain conditions, deep-lying acceptor states were produced. The temperature at which the Hall effects were measured moved the Fermi level through this restricted energy range. In CdS, two energy levels were identified by Chester: $0.049 \pm 0.001\text{eV}$ (hydrogenic level) below the conduction band, and $0.11 \pm 0.01\text{eV}$ below the conduction band. Three energy levels in CdTe were indicated by the analysis of the Hall results: $0.019 \pm 0.002\text{eV}$ (hydrogenic level), $0.065 \pm 0.003\text{eV}$, and $0.16 \pm 0.01\text{eV}$ below the conduction band. The most significant observation was the change in the nature of the effect as the energy of the incident gamma rays was changed. For example, ^{137}Cs photons introduce acceptors in CdS and donors in CdTe, which ^{60}Co photons produce just the reverse effect. Thermal neutron irradiation of both materials introduces only acceptors.

Chester concluded that a comparison of the calculated atomic displacement cross-sections with the observed energy level introduction rates indicates a possible correlation between the energy level introduced and the type of atom displaced in the compound. Irradiation of CdS with the 1.17- and 1.33-MeV ^{60}Co gamma rays results in an increase in the relative density of the 0.049eV hydrogenic donor centre. In CdTe, irradiation

with 0.662 MeV ^{137}Cs gamma rays results in an increase in the relative density of the 0.019 eV hydrogenic donor centre. Cross-section calculations indicate a preferential cadmium atom displacement in both cases. However, the density of hydrogenic donor level increases in the region where the cadmium atom displacement is preferable based on the cross-section calculations. In the case of preferential chalcogenide atom displacement, the total acceptor concentration increases. Therefore, the low energy ^{137}Cs photons should preferentially displace sulfur atoms in CdS and cadmium atoms in CdTe; the reverse is obtained for ^{60}Co irradiation.

A similar phenomenon is also observed in semiconductors bombarded by charge particles. If charged particles, such as electrons, protons, alpha particles, etc. bombard a binary semiconductor, generally both types of atoms will be displaced. If the two types of atoms have the same displacement threshold and if the incident particle energy is low (e.g. a few MeV), then the atom with the largest atomic number will have the greatest displacement cross-section. The scattering law for charged particles favours low energy transfer. The result is that single atom displacements predominate as in gamma ray irradiation; multiple atom displacements only occasionally occur. For example, in CdTe, both atoms are assumed in the calculations to have the same displacement threshold. In CdS, cadmium has a larger atomic number and therefore the larger displacement cross-section, and has the smaller displacement threshold. As a result, charged

particle bombardment should produce preferential Cd atom displacement in CdS and preferential Te atom displacement in CdTe. Thus, charged particle bombardment of CdS and CdTe would be expected to produce preferential donor introduction in CdS and acceptor introduction in CdTe.

2.3.2 Fluorescence in CdS

It has been recognized that there are several methods of producing vacancies and interstitials in materials. A common method employed is to heat the material to a temperature near its melting point, then to quench it to a low temperature. The major disadvantage of this method is that all the defects as well as the other impurities are able to diffuse rapidly through the material and hence, the configuration of the defects is not known. Another method is by irradiation with ultraviolet light or x-rays. A third method is by electron bombardment. If the electrons are of energy only slightly above the threshold for displacement of an atom from the lattice, then only one vacancy and one interstitial will be produced in a single collision. If the temperature is low enough, there will be no diffusion of the defects and it is possible to produce simple isolated vacancies and simple isolated interstitials. For a compound material consisting of two species such as CdS, it should be possible to observe two thresholds for displacement. Thus, by bombarding at energies between these two thresholds, defects of the lighter species may be produced, and by bombarding at energies above the higher threshold, defects of both species should be

produced. A further advantage of this method is that the number of defects produced can be controlled by controlling the number of electrons striking the sample.

A change in luminescence following radiation damage was observed by Reynolds and Greene (1958). Later, Collins (1959) observed the production of edge emission in CdS by electron bombardment at 200KeV at 77°K. Subsequently, Kulp and Kelly (1960) measured the threshold for the production of edge emission at 115KeV in a sample which did not originally show edge emission. This electron energy transfers a maximum of 8.7eV to the sulfur atom. In a sample which showed edge emission before bombardment, the edge emission was removed by bombardment with electrons in the energy range 2.5 to 200KeV. Kulp and Kelly also measured the change in resistivity due to irradiation. They found that the resistivity was increased by electrons with energy above a threshold (~115KeV). Kulp (1962) extended this work by irradiating CdS at 77°K. He found a 290KeV energy threshold for the production of two fluorescence bands (at 6050 and 10,500Å). Fig. 2.14 shows the fluorescence at 80°K of a crystal of CdS before and after bombardment at 500KeV obtained by Kulp. The bands at 6050Å and 1.03μ are intensified by bombardment above 290KeV. The other bands at 5150Å and 7200Å are those produced by electrons of energy greater than 115KeV. He associated the 6050Å (or 1.03μ) band with the Cd interstitial, and the 10,500Å (or 1.05μ) band with the Cd vacancy. He also found that an electron energy of 290KeV would transfer a maximum energy of 7.3eV to a cadmium atom. The value found

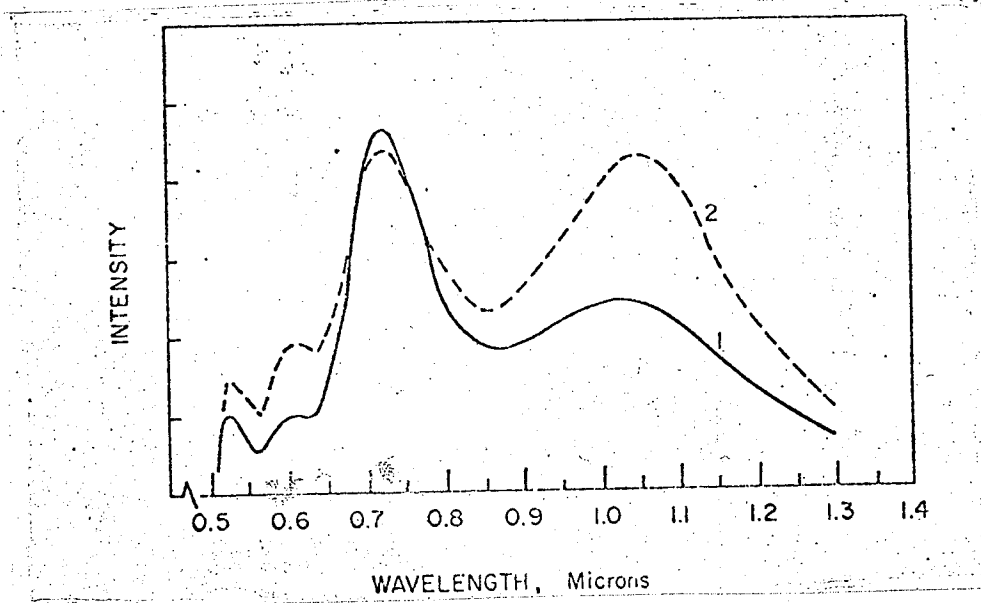


Fig. 2.14 Spectra of CdS at 80°K before (solid curve) and after (dashed curve) electron bombardment at 500KeV. (Kulp, 1962)

for the displacement energy for the sulfur atom in CdS was 8.7eV. Thus, it appears that the cadmium atom is bound somewhat less strongly than the sulfur atom. Kulp also noted that the fluorescence bands appeared and disappeared as the temperature was cycled and as the bombardment progressed, and he concluded that each of the centres produced by the bombardment experiments must exist in more than one ionization state. The particular state of ionization of each defect is determined by the position of the Fermi level. This is sensitive to the total number and type of impurities in the crystal and hence varies greatly from crystal to crystal. The time required for obtaining the steady state condition is often rather long. Quasi steady state conditions might be expected to exist during and following the periods of heavy ionization caused by electron bombardment which can cause a change in the distribution of the electrons over the existing defects. Temperature cycling or long decay times or both may be required before a return to equilibrium is accomplished. Kulp suggested that the electron bombardment near the thresholds for displacement of the cadmium and sulfur atoms offers a new approach to the problem of the effect of radiation; however, the results obtained are very complicated.

In a subsequent experiment (Schulze and Kulp, 1962), a group of crystals of CdS whose dark conductivity was of the order of $10^{-8} \sim 10^{-10}$ ($\Omega\text{-cm}$)⁻¹ were bombarded with electrons in the energy range from 25 to 125KeV.

After bombardment, the dark conductivity changed to a value of the order of $10^{-3}(\Omega\text{-cm})^{-1}$. They also found that the crystal could be returned to the original conductivity by an appropriate heat treatment. The temperature at which the conductivity began to decrease varied from 30° to 200°C . By stopping the heat treatment just as the conductivity began to decrease, it was possible to return the crystal to its original conductivity in a series of steps. The storage effect is the result of an irreversible redistribution of the electrons and holes over the existing defects. Schulze and Kulp attributed the large persistent conductivity increase produced by electron-irradiation to a redistribution of electrons and holes among already existing levels, and not to the production or removal of defects.

2.3.3 Fast-Neutron Irradiation Effects in CdS

Some of the effects of fast neutron irradiation in CdS have also been investigated recently. Oswald and Kikuchi (1965) irradiated low resistivity crystals and found that the resistivity increased with fast neutron irradiation dose. Subsequently, Galushka (1966) irradiated high resistivity crystals with fast neutrons and observed that the resistivity decreased. According to these results, Johnson (1968) suggested that the resistivity of CdS may approach a limiting value upon irradiation with fast neutrons. In his study, both low resistivity crystal (LRC) and high resistivity crystal (HRC) of CdS were irradiated in the same reactor environment. In order to avoid contact effects, the changes in the resistivity and Hall mobility resulting from the irradiation were measured using

four-terminal techniques. As a result of fast neutron irradiation, Johnson found that the Hall mobility decreases by 3% - 5% at 10^{14} neutrons/cm² and 20% - 30% at 10^{17} neutrons/cm². Initial carrier removal rates are dependent on the initial carrier concentrations and vary from positive values for the LRC to negative values for the HRC. The resistivity of the irradiated LRC increases with fast neutron fluence while that of the irradiated HRC decreases. After continuous irradiation to fluences $>10^{17}$ neutrons/cm² for 24 hours, the resistivity of the crystals approaches a limiting value of $\sim 2 \times 10^4 \Omega \cdot \text{cm}$, independent of the initial resistivity. The corresponding limiting position of the electron quasi-Fermi level is at $\sim 0.37 \text{ eV}$ below the conduction band and is determined by the induced effects and ionization effects resulting from the decay of radioactive products. Following irradiation, Johnson found that three separate time-dependent processes occur, which cause changes in the resistivity. Two of these are temperature-independent and follow first-order kinetics with half-lives of ~ 1 and ~ 14 days, respectively. The third process is much slower and is temperature-dependent. He concluded that initial changes in the post-irradiation resistivities are primarily results of the first two processes and are attributed to self-ionization of the sample by radio-active decay of transmuted atoms produced during the irradiation.

2.3.4 The Change of Electrical Properties by Thermal Treatment in ZnSe

Woodbury and Aven (1965) have discussed the effects of electron irradiation and thermal treatments on the electrical transport properties of n-type ZnSe crystals. Their results given in Fig. 2.15 show the temperature dependence of the Hall coefficient and the Hall mobility for a Cl-doped ZnSe crystal fired in liquid Zn. They called the conditions of the crystal after the 850°C and the 1050°C thermal treatment to be the annealed state and fired state respectively. They found that in the annealed state the freeze-out of carriers occurs on a donor level approximately 0.02eV below the conduction band edge. In the fired state, in addition to the shallow level, a level 0.16eV below the conduction band edge was obtained. When the crystal is illuminated with incandescent light at temperatures below approximately 100°K, the electrons frozen into the 0.16eV level are released, producing an increase in carrier concentration as shown by the dashed curve in Fig. 2.15. The increase in carrier concentration persists even after the illumination is discontinued as long as the crystal is kept at low temperatures. According to their experimental results of the Hall mobility and Hall coefficient, Woodbury and Aven concluded that the 0.16eV level is the second charge state of a double acceptor. When a region in a crystal containing such a level is illuminated at low temperatures with radiation capable of producing electron-hole pairs, the holes are quickly captured by the double acceptor centres, which are negatively charged, leaving them in the -1 charged state. Because of the Coulombic repulsion between these centres and the electrons in the conduction band, the re-

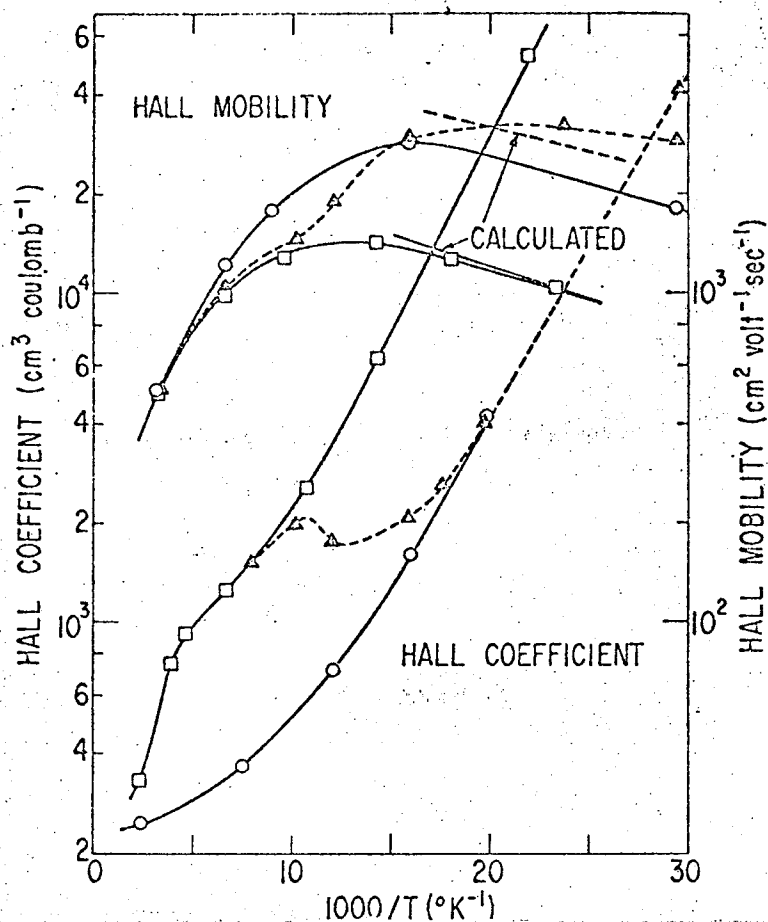


Fig. 2.15

Temperature dependence of Hall mobility and Hall coefficient for a Cl-doped ZnSe crystal fired in liquid Zn. Solid lines indicate measurements performed in the dark, dashed lines under illumination, circles after 850°C firing, squares and triangles after 1050°C firing. (Woodbury and Aven, 1960)

combination of the created electron-hole pairs via the double acceptor centre is very slow. The result is a persistent increase in carrier concentration. The reduction of the charge state of the double acceptor centres from -2 to -1 under illumination also significantly reduces the scattering of the electrons in the conduction band, leading to the observed increase in the low temperature mobility. The satisfactory agreement between the calculated and observed mobilities gives quantitative confirmation of the 0.16eV level for the double acceptor centres.

2.3.5 Threshold Energies for Electron Radiation Damage in ZnSe

The threshold energies for the production of various fluorescence bands at different temperatures in ZnSe have been studied by many investigators. Kulp and Detweiler (1963) reported on the threshold energy for displacing an atom from the ZnSe lattice by electron bombardment. Fig. 2.16 shows the fluorescence of ZnSe at 80°K before and after bombardment by 500KeV electrons. Also, the rate of increase of the fluorescence as a function of electron energy for bombardment at 80°K is shown in Fig. 2.17. Since this rate of increase is proportional to the cross-section for displacement, Kulp and Detweiler found that the intercept with the energy axis in Fig. 2.17 at 240KeV is the threshold for displacement of an atom from the ZnSe lattice at 80°K. They also found that an electron of 240KeV transfers a maximum energy of 8.2eV to the selenium atom and 10eV to the zinc atom. No other threshold has been observed when bombarded at liquid-

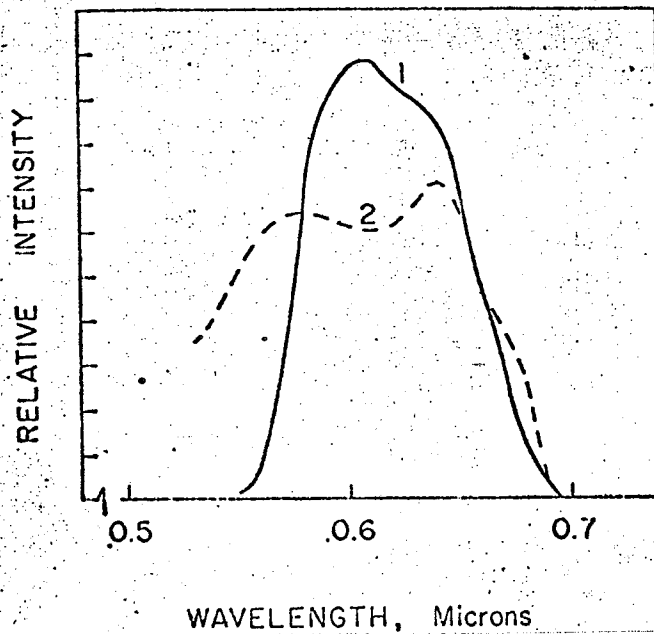


Fig. 2.16

Spectra of ZnSe at 80°K before (solid line) and after (dashed line) electron bombardment at 500KeV. (Kulp and Detweiler, 1964)

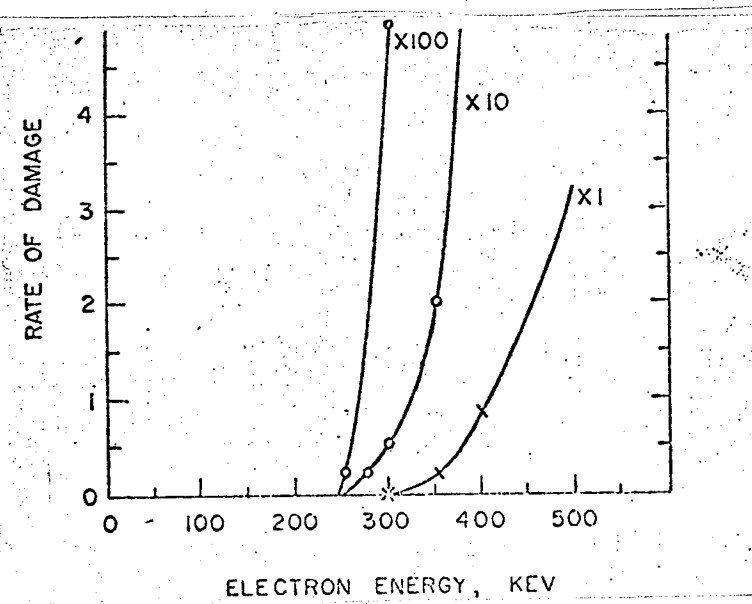


Fig. 2.17

Rate of increase in fluorescence at 80°K in ZnSe as a function of electron energy. Note expansion of intensity by factors of 10 and 100. (Kulp and Detweiler, 1964)

nitrogen temperatures. The radiation damage produced at 80°K anneals essentially in a single stage at about 130°K. In fact, not all ZnSe shows radiation damage through fluorescence at 80°K. Those crystals showing damage at 80°K are called type-I ZnSe, while those that do not are called type-II ZnSe. However, when bombarded at liquid-helium temperatures, both types of ZnSe show damage. When the crystal is bombarded by electrons at this temperature, the various stages of annealing would be observed. Fig. 2.18 shows the fluorescence spectrum of type-II ZnSe bombarded at 350KeV. The rate of increase of fluorescence as a function of electron energy for bombardment at liquid-helium temperatures is shown in Fig. 2.19. The results indicate the existence of a second threshold (195KeV) for radiation damage at liquid-helium temperatures in ZnSe crystals. Detweiler and Kulp (1966) found that the damage produced at liquid-helium temperatures (~10°K) annealed in several stages: the first at about 60°K, another at about 90°K, and the final at about 135°K. The energy transferred to the zinc atom is found to be 7.8eV and to the selenium atom is 6.2eV for a 195KeV electron. The difference of the displacement energy for the two constituent atoms in ZnSe is much larger than that in any other II-VI compound semiconductors. Furthermore, Detweiler and Kulp associated the threshold energy of 195KeV at 10°K with the zinc atom with a displacement energy of 7.8eV, and the threshold at 240KeV with displacement of the selenium atom with an energy transferred of 8.2eV. It is reasonable to assume that at low temperatures, simple isolated vacancies and interstitials are formed by the moderately low energy electrons.

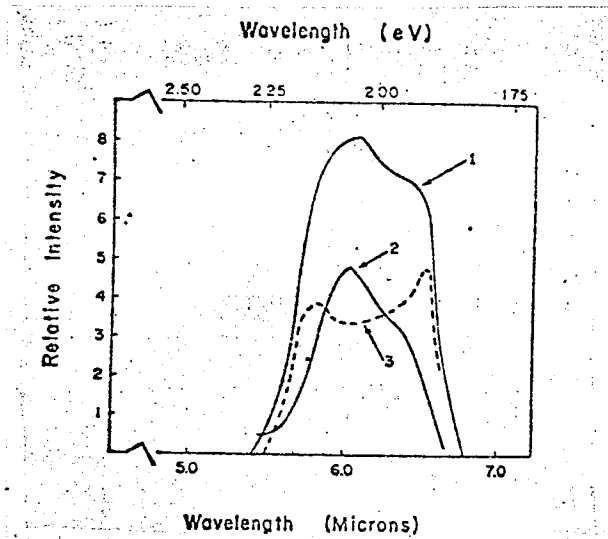


Fig. 2.18

The fluorescence spectrum of type II ZnSe bombarded at 350KeV at 10°K (curve 1). Curve (2) is the fluorescence of this crystal at 10°K after the 60°K anneal. Curve (3) is the difference between curves (1) and (2). (Detweiler and Kulp, 1966)

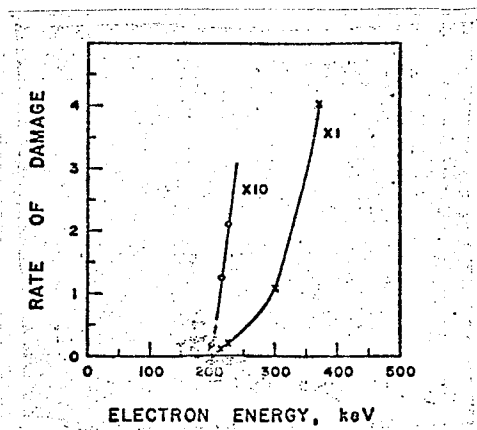


Fig. 2.19

The rate of radiation damage in ZnSe versus electron bombardment energy. Note expansion of intensity by factor of 10. (Detweiler and Kulp, 1966)

2.3.6 Photoelectronic Evaluation of Electron Radiation Damage in CdS

Recently, the full spectrum of photoelectronic techniques to analyze the effects of radiation damage in the II-VI compounds has been suggested by Ho and Bube in 1968, and these techniques have been used to investigate the electron radiation damage in CdS for electrons with energy between 75KeV and 2MeV. They found that the significant effect of electron radiation damage is to decrease the electron lifetime in high resistivity photosensitive crystals if the electron energy is 400KeV or higher. However, low temperature annealing of irradiated crystals under illumination removes the effects of damage on the electron lifetime although all irradiated crystals exhibit a distinctly different trap distribution from non-irradiated crystals.

CHAPTER III

THEORY OF RADIATION EFFECTS

Radiation effects may be classified into two types: transient and permanent. Transient effects may be defined as changes in operational properties that are noted during an irradiation, but which disappear when the radiation field is removed. Permanent effects begin during an irradiation but persist after it has ended (Kircher and Bowman, 1964). The scope of this thesis is limited to permanent effects on semiconductors. There are several types of radiations in the nature. It may be either corpuscular such as alpha particles, beta particles, protons, and neutrons, or electromagnetic, such as gamma rays or x-rays.

Gamma rays are high-energy photons and as such carried no charge or mass. At comparatively low energies, the photon can only eject weakly bound electrons surrounding an atom of a crystal. As the photon energy increases, it can eject more strongly bound electrons, and very high-energy photons interact with the atomic nucleus. Therefore, most damage due to gamma rays is the result of three types of interactions: the photoelectric effect, the Compton process, and pair production.

In the photoelectric process, a photon is completely absorbed in a collision with an electron and the electron is ejected from the atom. This can happen whenever the energy of the photon is greater than the binding energy of the electron. Then, the kinetic energy of the ejected electron

is given by

$$T = h\nu - E_B \quad (3.1)$$

where ' $h\nu$ ' is the photon energy and ' E_B ' is the binding energy of the electron. As the photon energy increases, more tightly bound electrons are ejected. The probability for interaction with a given electron is greatest when the energy of the photon is just slightly greater than the binding energy of the electron. If the photon energy continues to increase, it becomes increasingly difficult for the electron to carry away all of the photon energy and the importance of this process decreases while the importance of other processes increases. By approximation, the photoelectric absorption coefficient (τ) is proportional to $(h\nu)^{-3}$ and is also proportional to Z^3 where ' Z ' is the atomic number of the material.

In the Compton process, part of the photon energy is transferred to the electron in an elastic collision between a photon and an electron and the photon is scattered through an angle ' ϕ ' with reduced energy. The energy lost by the photon appears as kinetic energy of the electron and momentum is conserved in the collision. As the energy of primary photon increases, the probability of electron scatter in the forward direction will increase. When the Compton absorption coefficient is considered, it is important to note that the total Compton coefficient (σ_t) is the sum of

the true absorption coefficient (σ_a) which represents the energy given to the electron and thus truly absorbed and the scatter coefficient (σ_s) which represents the energy carried away by the scattered photon. The total Compton absorption coefficient can be expressed as follows: (Klein and Nishina)

$$\sigma_t = \frac{2\pi q^4}{m^2 c^4} \left\{ \frac{1+\alpha}{\alpha^2} \left[\frac{2(1+\alpha)}{1+2\alpha} - \frac{\ln(1+2\alpha)}{\alpha} \right] + \frac{\ln(1+2\alpha)}{2\alpha} - \frac{1+3\alpha}{(1+2\alpha)^2} \right\} \quad (3.2)$$

where 'm' is the rest mass of an electron, 'c' is the light velocity and $\alpha = h\nu/mc^2$. It can be seen that ' σ_t ' decreases as the energy increases (Fig. 3.1).

When the photon energy exceeds a certain threshold ($2mc^2=1.022\text{MeV}$), the pair production process may occur. In this process, the photon interacts with the nucleus of an atom and disappears with production of a pair of positive and negative electrons. The difference between the threshold energy and the photon energy is carried away in opposite directions by the pair of particles as their kinetic energy. Thus, the pair production absorption coefficient (K) increases with photon energy.

Therefore, the absorption of gamma rays is generally attributed to these three main processes. The linear absorption coefficient is then given by

$$\mu = (\tau_{\text{phot}} + \sigma_{\text{comt}} + K_{\text{pair}}) \quad (3.3)$$

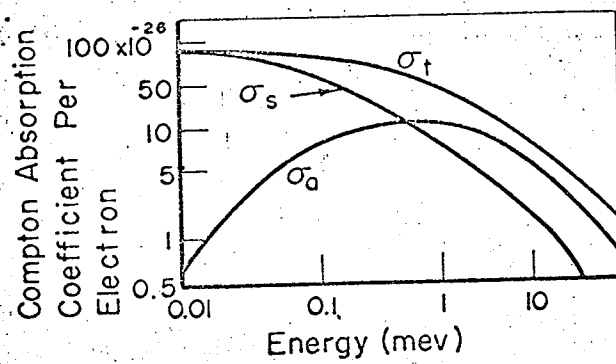


Fig. 3.1

Compton absorption coefficient per electron as a function of energy (σ_a : true absorption coefficient, σ_s : scatter coefficient, σ_t : total Compton absorption coefficient)

The intensity of the photon beam then can be written as

$$I = I_0 \exp(-ux) \quad (3.4)$$

The energy region over which the three primary processes predominate is shown in Fig. 3.2.

The electron is a negative charged particle with a mass 'm'.

A variety of processes are responsible for the loss of energy by an electron passing through matter. For energetic electrons, the important processes are collisions yielding ionized or excited atoms and electromagnetic radiation production. It has been seen that the energy absorbed from gamma rays gives rise to energetic electrons, and these electrons actually cause most of the changes in a material irradiated by gamma rays.

In the theory of ionization losses, developed in its modern form by Bethe (1953), the specific energy loss $-dE/dx$ (i.e. the rate of loss of energy) is given by

$$-\frac{dE}{dx} = \frac{2\pi Nq^4}{m V^2} Z \left[\ln \frac{mV^2 E}{2I^2(1-\beta^2)} - (2\sqrt{1-\beta^2} - 1 + \beta^2)\ln 2 \right. \\ \left. + 1 - \beta^2 + \frac{1}{8} (1 - \sqrt{1-\beta^2})^2 \right] \quad (3.5)$$

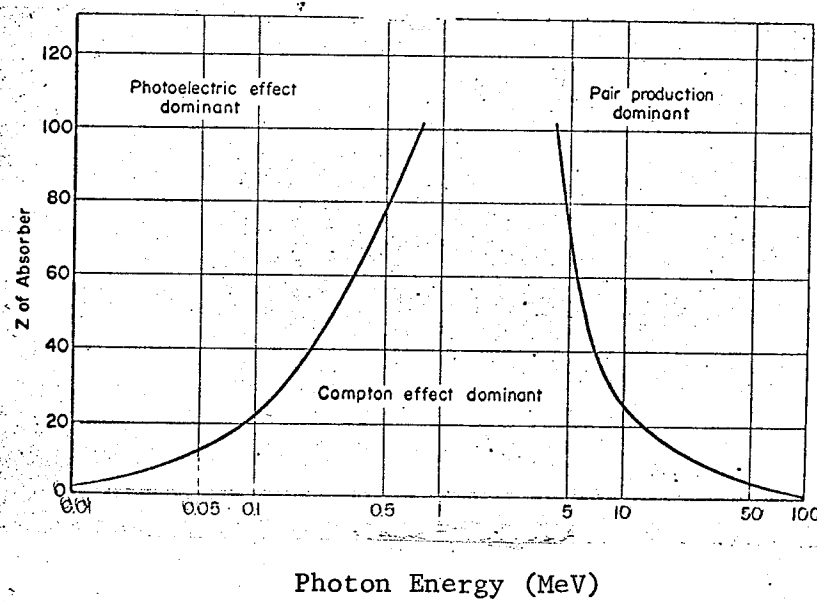


Fig. 3.2 Diagram showing the photo energies E and the crystal atomic numbers Z at which the principal γ -quantum absorption processes become dominant. (R.D. Evans, 1965)

where 'E' is the kinetic energy of a fast electron, 'V' is its velocity, $\beta = V/c$ ('c' is the velocity of light), 'I' is the average ionization potential or average energy of electron excitation, and 'N' is the number of atoms in a unit volume (1cm^3) of material through which the electron is travelling. For small values of ' β ', i.e. the velocity of the electron is much slower than the velocity of light, it becomes

$$-\frac{dE}{dx} = \frac{4\pi q^4 N}{m V^2} Z \ln \left(\frac{m V^2}{2I} \sqrt{\frac{e}{2}} \right) \quad (3.6)$$

where the 'e' under the logarithm is the natural base of logarithms from which it can be seen that the specific ionization is proportional to the atomic number 'Z' and inversely proportional to the energy of the primary electron.

Some electrons ejected during ionization will have sufficient energy to cause further ionizations. These energetic secondary electrons are called delta rays. Thus, the total ionization will be the sum of the ionization from the primary and secondary electrons or delta rays.

Neutrons are uncharged particles and hence can penetrate the electron cloud of an atom and interact with the nucleus. As a result, the nucleus can be moved from its position, and most of the chemical and physical changes in materials which result from neutron bombardment are a result of this process of elastic scattering. The energy transferred to

the struck atom in an elastic collision is given by

$$E = \frac{4M}{(M+1)^2} E_n \cos^2 \theta \quad (3.7)$$

where 'M' is the mass of recoil atom, ' E_n ' is the energy of the neutron, and ' θ ' is the recoil angle of the nucleus. It can be seen that the energy transferred to recoil atom is inversely proportional to the mass of the recoil atom.

If the neutron scattering can be assumed to be isotropic, all recoil energies between zero and ' E_{\max} ' are equally probable. The average energy transferred in a collision is $\bar{E} = E_{\max}/2$. It should be noted that the average energy of recoil atoms resulting from bombardment with fast neutrons is many times greater than the average energy of recoil atoms resulting from bombardment with heavy charged particles (e.g. alpha particles, protons) due to their different scattering processes.

The recoils from elastic collisions sometimes have sufficient energy to produce other recoils. The primary knocks out atoms so that the final total number of defects is always considerably greater than the number of collisions between the incident fast neutrons and atoms in the crystal. The end result is the creation of imperfection in the lattice.

At low energies, neutrons will not be able to displace atoms but they can be captured by nuclei. Low energy neutrons are generally absorbed

by radiative capture in which the nucleus is left in an excited state and returns to the ground state by emission of gamma rays.

The radiation damage to semiconductors generally results from a disruption of the crystalline structure of the crystal. Any deviation from a perfect crystal lattice can be considered as a defect and the interpretation of radiation effects centres around the production of various types of defects. The more important types of defects are vacancies, interstitials, impurity atoms, thermal spikes, and ionization effects. But, the most important defects considered for II-VI compound semiconductors are vacancies, interstitials and ionization effects. Vacancies created by collision of energetic particles with atoms of the lattice. The recoiling atom (knock-on) generally has sufficient energy to create other vacancies, giving rise to a cascade of defects. When recoiling atoms stop in some non-equilibrium position of the lattice, interstitial defects may result. Ionization effects result from the passage of charged particles or gamma rays through a material. As described above, the most important effect of gamma rays is the production of electrons which in turn produce interstitials and vacancies.

Threshold displacement energy, which is the minimum energy to remove an atom, is one of the most important subjects for studying the radiation effects on semiconductors. Some experimental results of threshold energy for II-VI compounds have been discussed in the previous Chapter.

To study the effect of radiation, the electrical conductivity and Hall effect are usually the properties to be experimentally studied, from which the mobility and concentration of charge carriers can be determined. Carrier concentration is very sensitive to lattice imperfections which can trap electrons in their neighbourhood and introduce energy levels for localized electrons. These energy levels can be either donor or acceptor levels, and one imperfection centre may introduce more than one level. According to James and Lark-Horowitz, vacancies produce acceptors and interstitials give donor levels. The mobility of carriers is decreased and scattering is increased by the defects introduced into the lattice as a result of irradiation.

CHAPTER IV

EXPERIMENTAL METHODS AND RESULTS

4.1 Experimental Apparatus and Procedures

In order to study the effects of gamma ray radiation on ZnSe single crystal, the following characteristics of the crystals were measured before and after irradiation: the dark resistivity, the voltage-current (V-I) characteristics and the Hall mobility of the majority carriers under various temperatures. The circuit which was used for these measurements is illustrated in Fig. 4.1. Since the resistivity of the sample is very high, the Hall effect measurement would be affected by any noise signal in the laboratory, and therefore all measurements were performed in a double screen room. With a proper common ground, all voltages were measured by an electrometer with an input resistance of the order of 10^{14} ohms. This instrument's noise level is about $2\mu\text{V}$. The currents were measured by a mirror galvanometer which provides a scale down to 10^{-12} amperes. A Varian electromagnetic unit which produces a magnetic field in the range from 0 to 15KGauss was used for Hall effect measurement. The sample holder for Hall effect and conductivity measurements from room temperature down to liquid nitrogen temperature (-196°C or 77°K) is shown in Fig. 4.2 and the details of the specimen holder in Fig. 4.3. The holder was placed in between the magnetic poles and the centre line of the magnetic poles was set to be perpendicular to

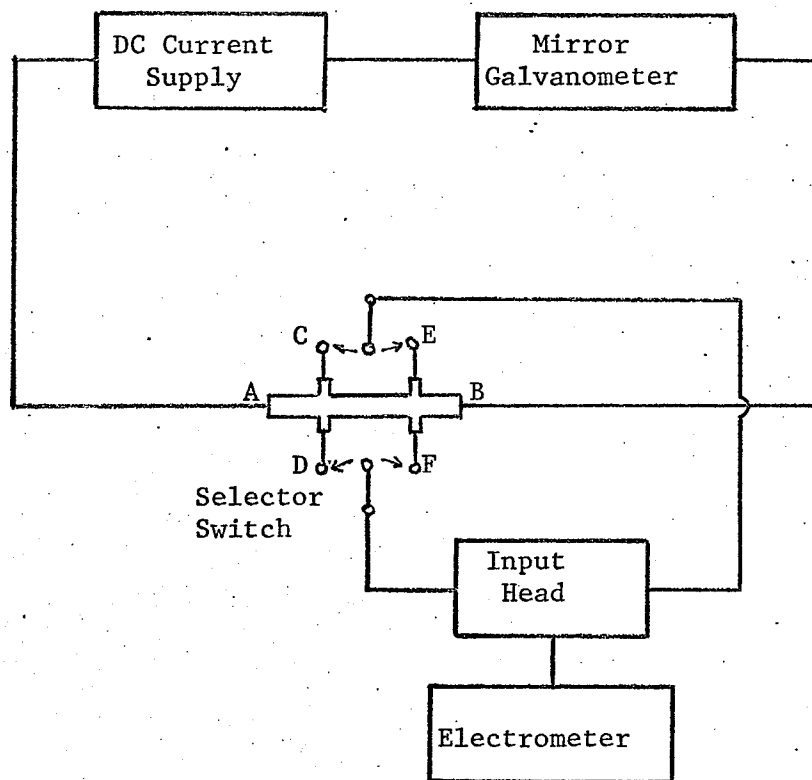


Fig. 4.1 *Circuit arrangement for Hall Effect and Conductivity Measurements*

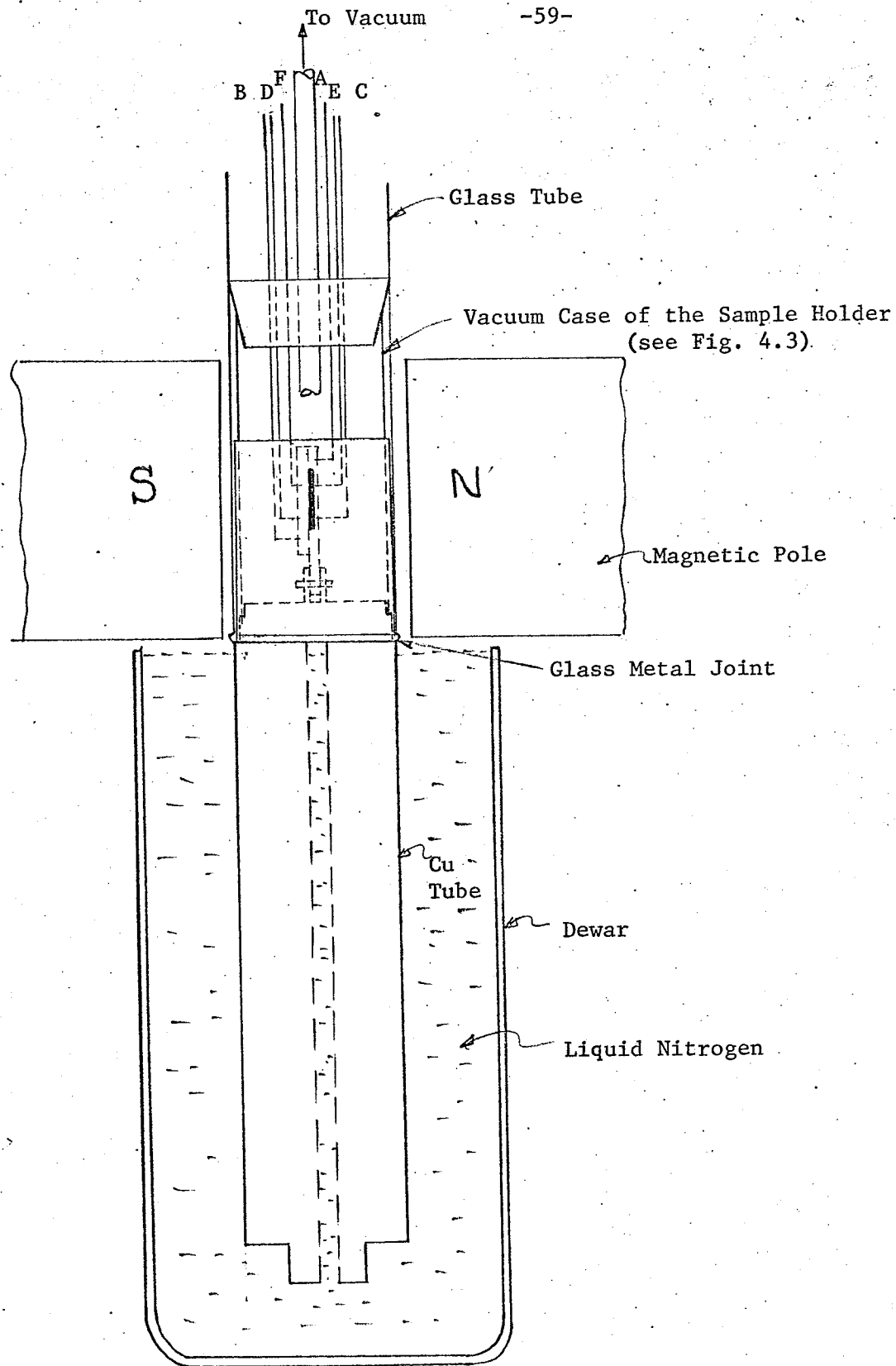


Fig. 4.2 Apparatus for Hall Effect and Conductivity Measurements for temperatures down to 77°K

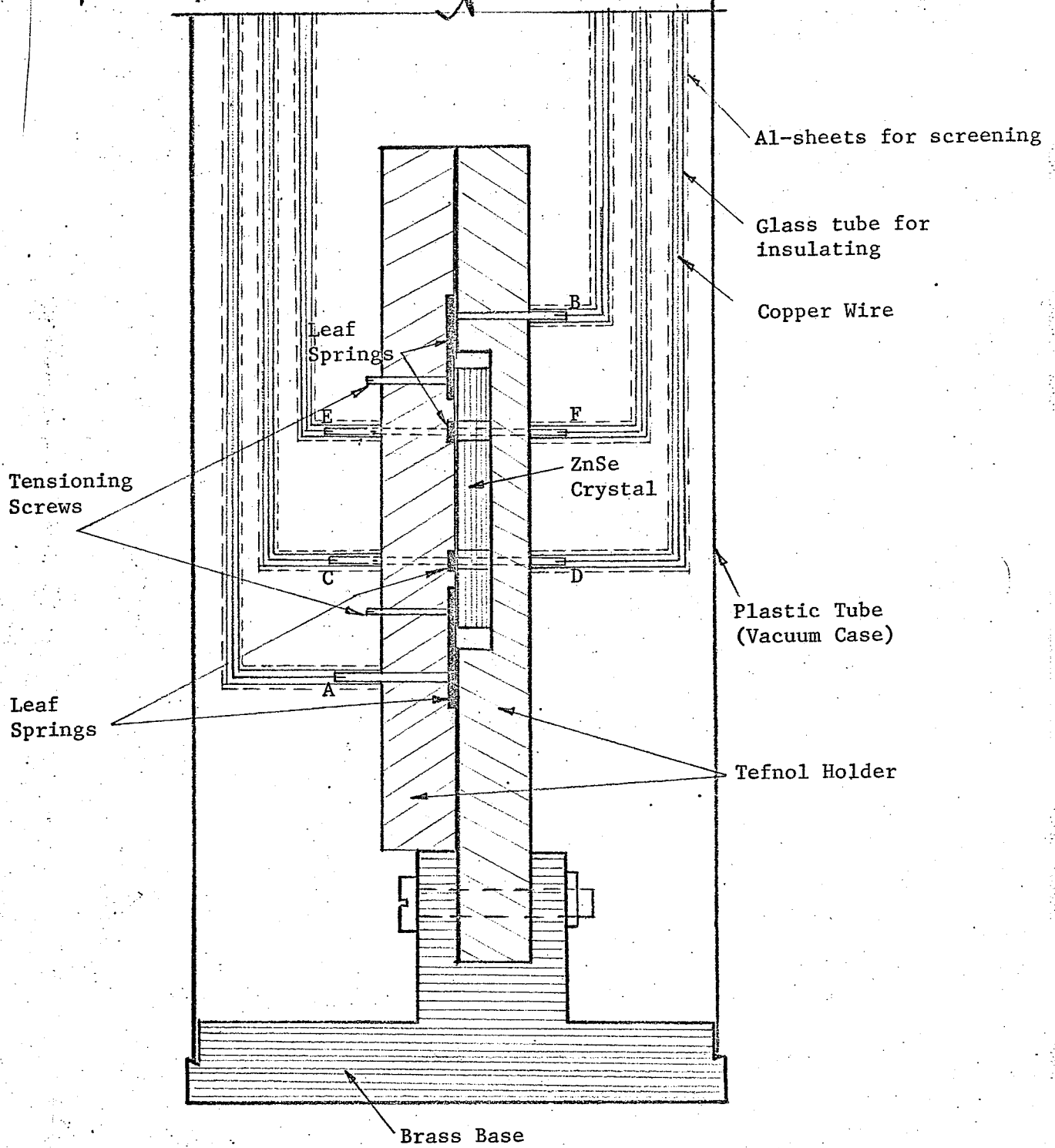


Fig. 4.3 Sample Holder for Hall Effect and Conductivity Measurements

the geometric centre of the sample, which provides a maximum magnetic flux across the specimen. Because of the sensitive photoconductivity of the ZnSe crystal, the sample holder was screened completely by aluminum sheets. Thus, all the measurements can be considered to be made in the dark.

The sample of undoped ZnSe crystal was supplied by Harshaw Chemical Company. The geometry and dimension are shown in Fig. 4.4. Indium electrodes have been affixed on the sample, and the contacts were made to be ohmic. The sample was provided with five pairs of contacts (A-B, C-D, E-F, C-E, and D-F). The current was supplied through the large contacts at each end (i.e., A and B). The electrodes along the sample on both sides are contacts for the Hall and conductivity measurements, the ones opposite each other across the specimen (C-D and E-F) for Hall effect measurements, while the ones along the length of the sample on the same side (i.e., C-E and D-F) for voltage measurements. The sample resistivity was obtained by dividing the averaged voltage developed between the pair of probes along the sample on both sides (C-E and D-F) by current 'I' according to the following relation

$$\rho = \frac{V_{IR} \cdot d \cdot W}{I \cdot L} \quad (4.1)$$

where 'd' is the thickness of the sample, 'W' is the width, and 'L' is the arms separation at the same side of the specimen. 'I' is the current averaged in both directions and ' V_{IR} ' is the average potential between the probes in these two measurements.

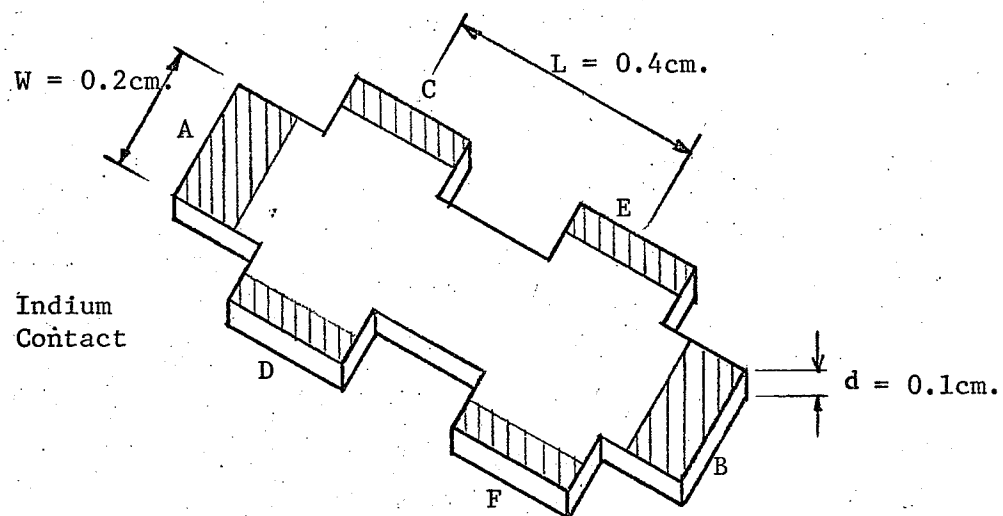


Fig. 4.4 Geometry and Dimensions of the ZnSe Sample

Careful Hall effect measurements were made over a wide range of temperatures. In the absence of a magnetic field, there may be a voltage between those Hall probes (i.e. C-D or E-F) owing to their imperfect alignment. This error can be eliminated by reversing the magnetic field and taking the averaged potentials. The error introduced by thermal-electric effects if the temperature of the specimen is not uniform can be eliminated by reversing the current and taking the averaged voltages again. By taking the average of these readings, all errors could be eliminated. Hence, the standard technique for reversing both magnetic field and current was used. The Hall coefficient R_H is given by

$$R_H = \frac{V_H \cdot d \cdot 10^8}{I \cdot H} \quad (4.2)$$

where ' V_H ' is the average of the eight Hall voltages [$V_{C-D}(\pm B, \pm I)$, $V_{E-F}(\pm B, \pm I)$], and ' H ' is the strength of the magnetic field normal to the current.

Then, the Hall mobility can be calculated from the Hall coefficient and the resistivity

$$\mu = \frac{R_H}{\rho} = \frac{V_H \cdot L \cdot 10^8}{V_{IR} \cdot W \cdot H} \quad (4.3)$$

If, in Eqn. 4.1, ' I ' and ' V_{IR} ' are measured in practical units, the resistivity ' ρ ' will have the dimension ohm-cm. If the magnetic field of strength ' H ' is measured in Gauss in Eqn. 4.2, the Hall mobility ' μ ' will have the dimension $\text{cm}^2/\text{V-sec}$.

Copper constantan thermocouples were used for measuring the temperature of the sample. It has been assumed that the conditions are isothermal; that is to say that no temperature gradient exists in the sample being studied.

The gamma irradiation was conducted in a cobalt ^{60}Co gamma cell with a half lifetime of 5.27 years and an average dose rate of 1.2×10^6 rads/hr, determined by ferrous sulphate dosimetry method. The temperature of the ^{60}Co gamma cell was about 35°C (irradiation temperature).

4.2 Experimental Results

All the experimental results are presented in this section and discussed in the next chapter. Fig. 4.5 shows the voltage dependence of the dark current for the ZnSe sample at fields from 0 to 1kV/cm (0-400V) for two temperatures before irradiation. Fig. 4.6 shows the voltage dependence of dark current for the crystal before and after irradiation with various doses of ^{60}Co gamma rays. The current increases with electric field, and this increase becomes more rapid for fields larger than 0.5kV/cm . All the curves are similar in shape, but the current decreases as the radiation dose increases.

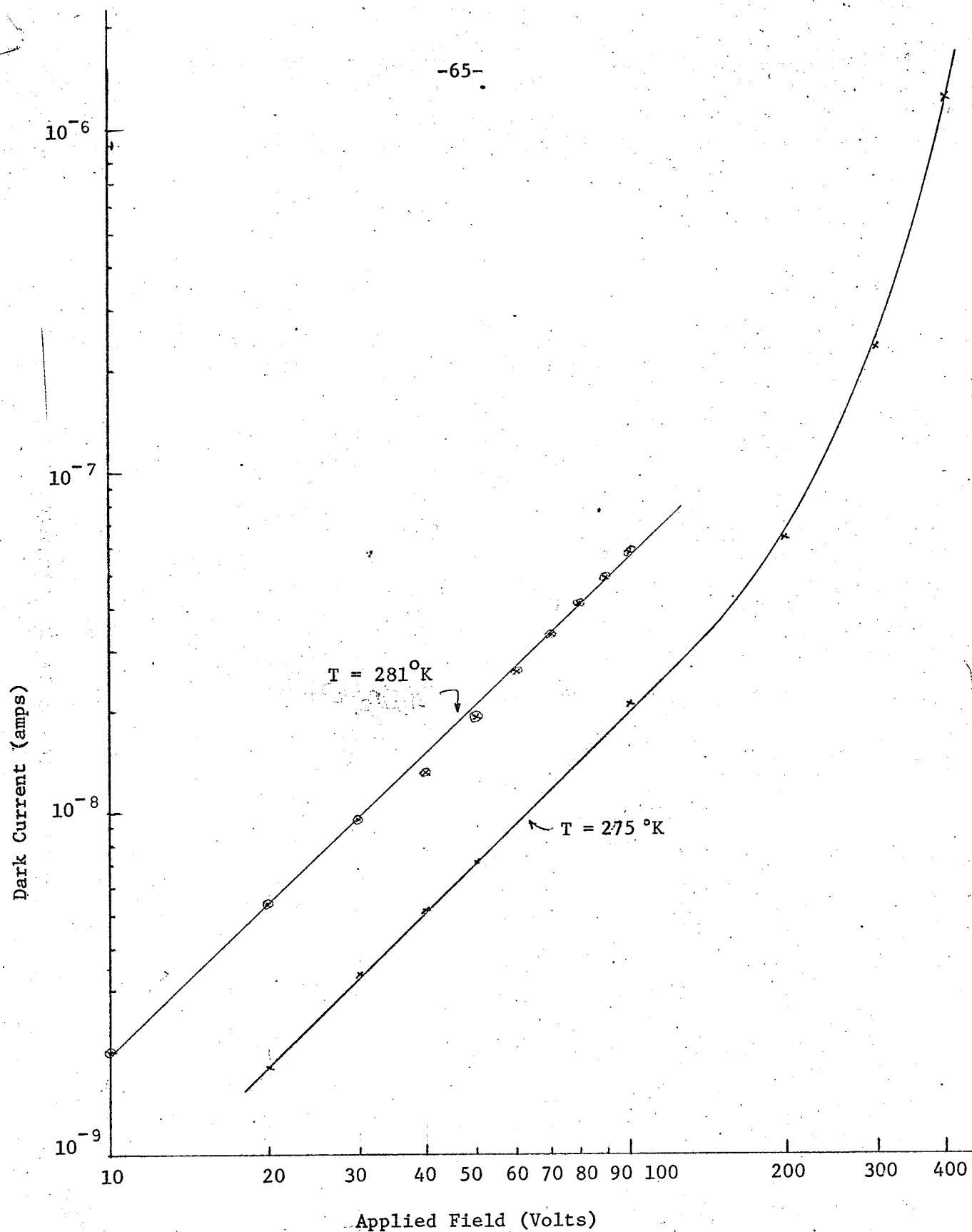


Fig. 4.5 The Voltage Dependence of Dark Current in ZnSe Single Crystal before Irradiation

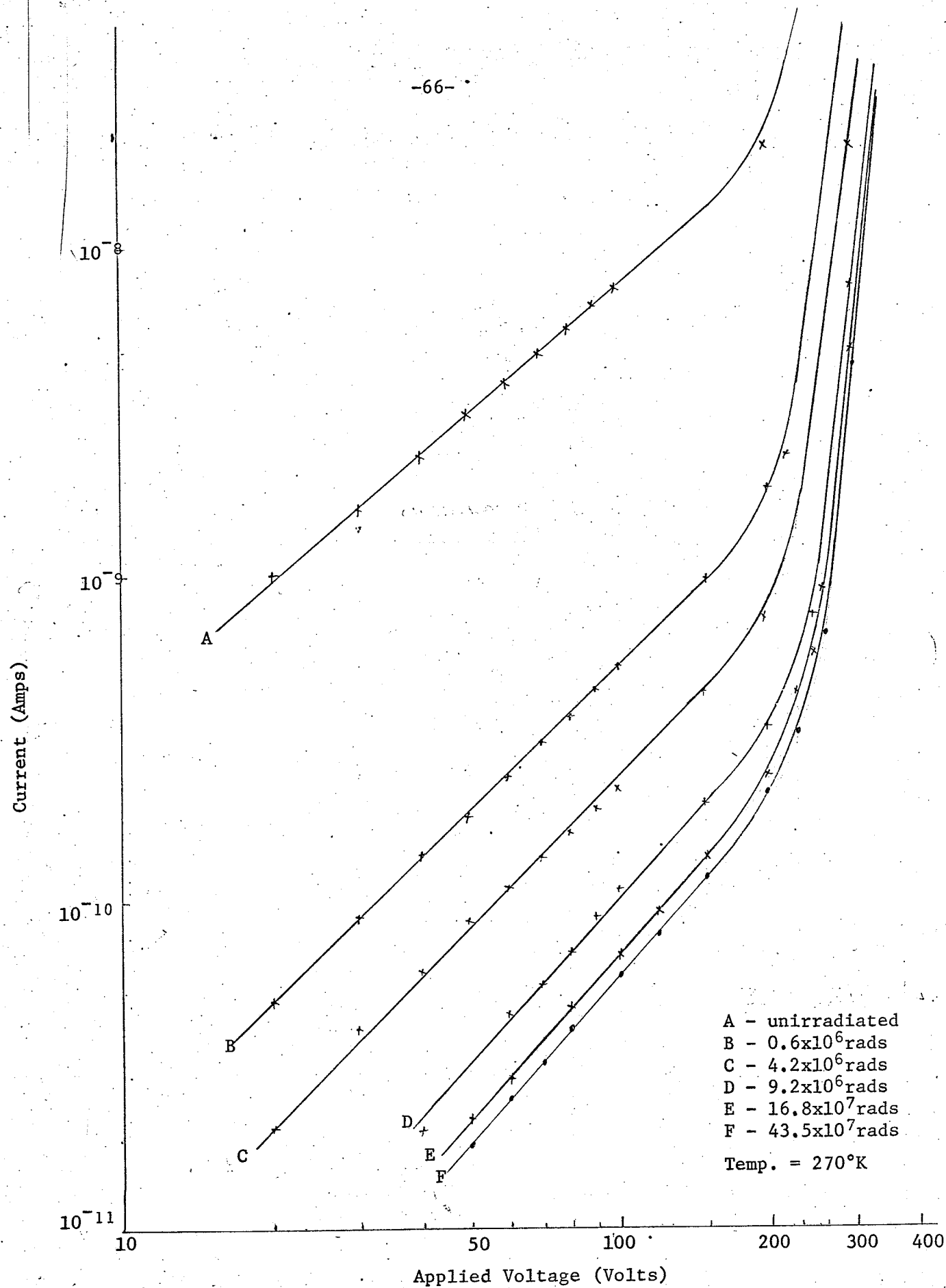


Fig. 4.6 The Voltage Dependence of Dark Current before and after Irradiation with Gamma Rays.

The results of the temperature dependence of resistivity with three different applied voltages (50V, 200V and 400V) without and with irradiations are plotted in Figs. 4.7, 4.8 and 4.9. Because of the limitation of the instrument, the temperature range in all these measurements was limited to approximately 180°K to 300°K. The resistivity of the ZnSe crystal as a function of radiation dose is shown in Fig. 4.10.

The Hall mobility was measured in a wider range of temperatures (84°K to 300°K). A magnitude of 4000 Gauss of magnetic field has been used in the Hall effect measurement. The Hall mobility as a function of temperature before and after gamma radiation is given in Fig. 4.11, and that as a function of radiation dose in Fig. 4.12.

The temperature dependence of the Hall coefficient can be calculated from the Hall voltage, the current through the crystal, and the applied magnetic field, and it is shown in Fig. 4.13 for the cases before and after gamma radiation.

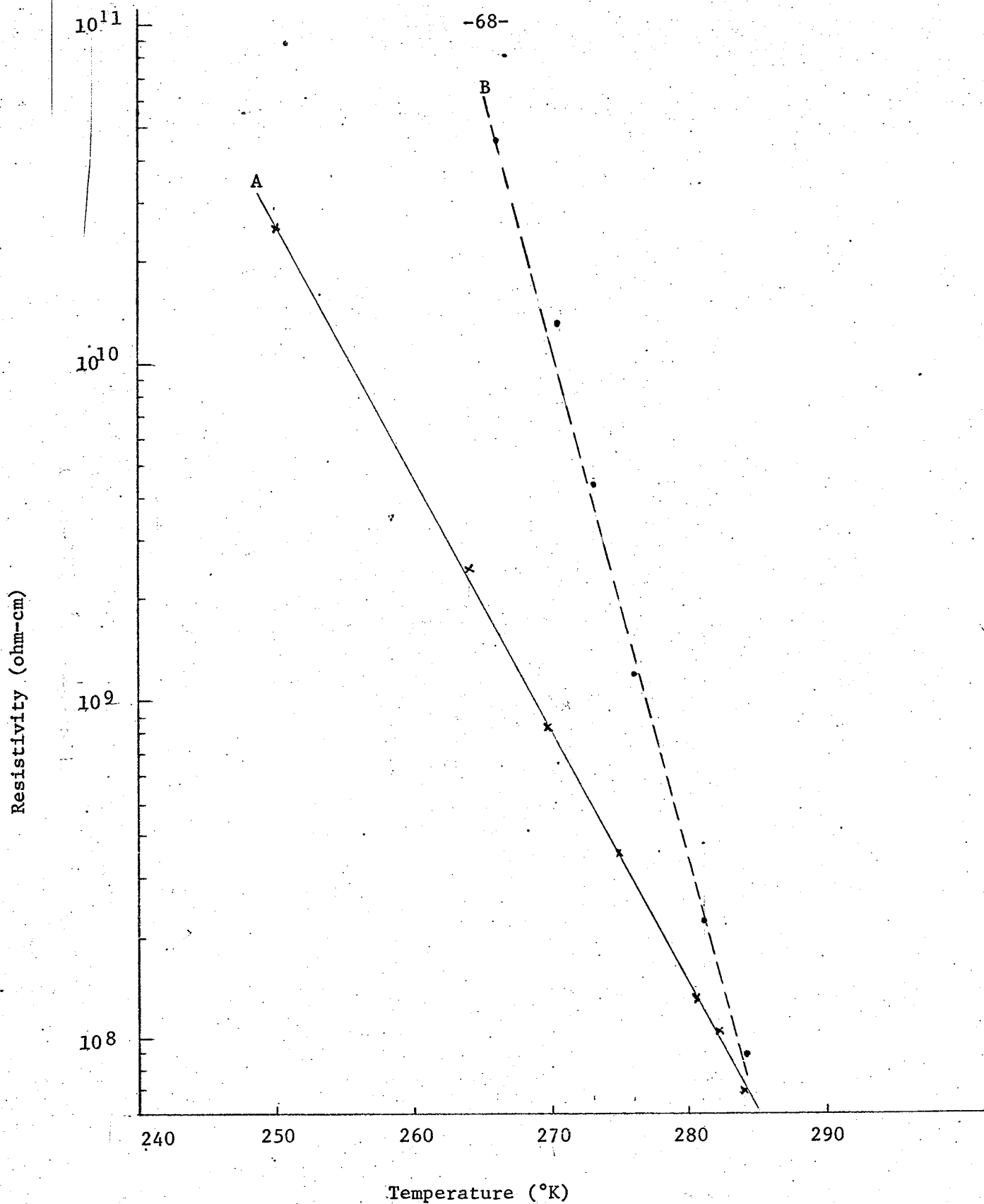


Fig. 4.7 The Temperature Dependence of Resistivity for a ZnSe Crystal before (solid line) and after (dash line) irradiation with Gamma Rays 0.6×10^6 rads. Applied Voltage = 50V. Magnetic Field = 0 Gauss.

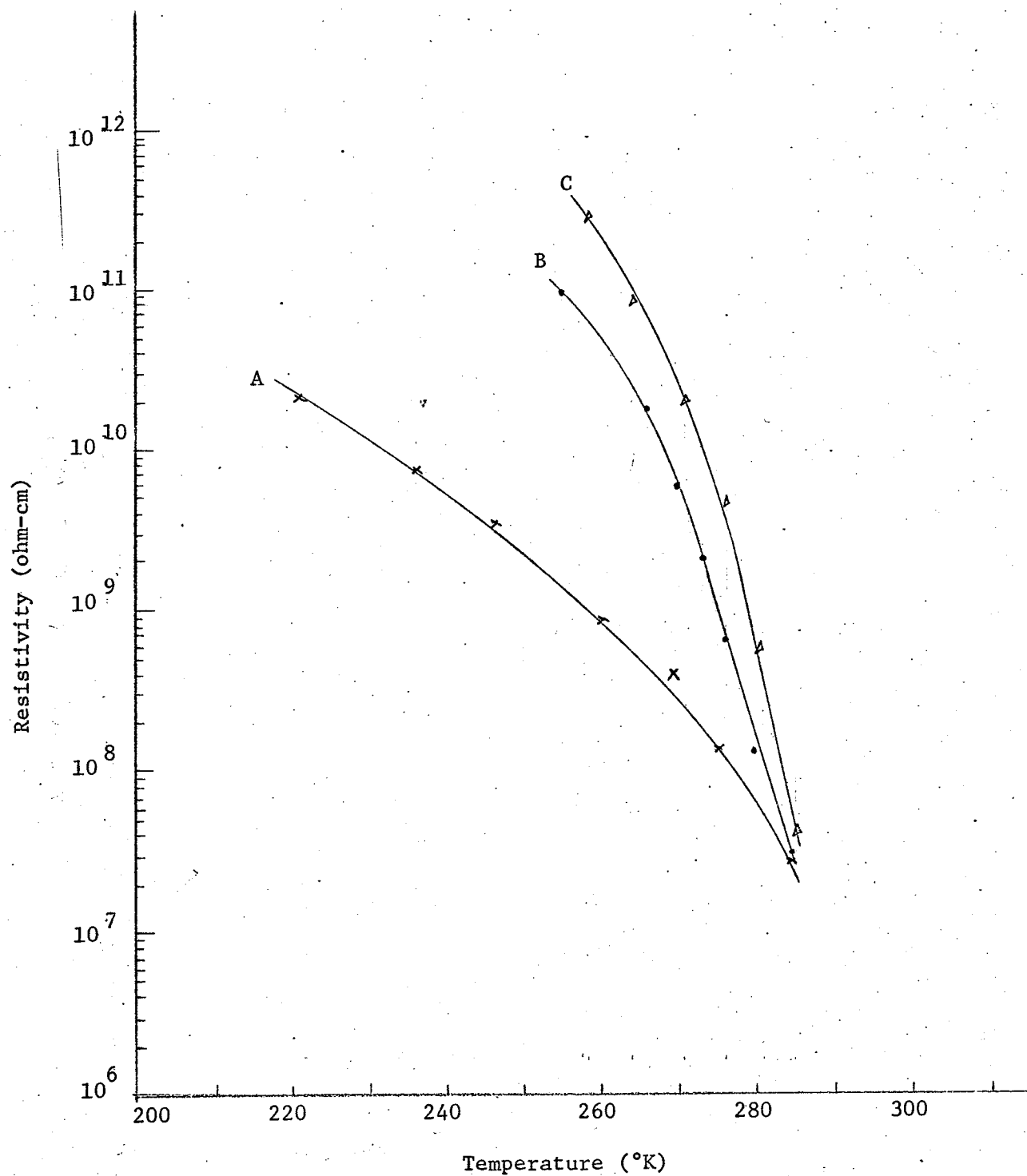


Fig. 4.8 The Temperature Dependence of Resistivity before (crosses) and after (solid circles: 0.6×10^6 rads.; triangles: 4.2×10^6 rads.) Irradiation with ^{60}Co Gamma Rays. Applied Voltage = 200V. Magnetic Field = 0 Gauss.

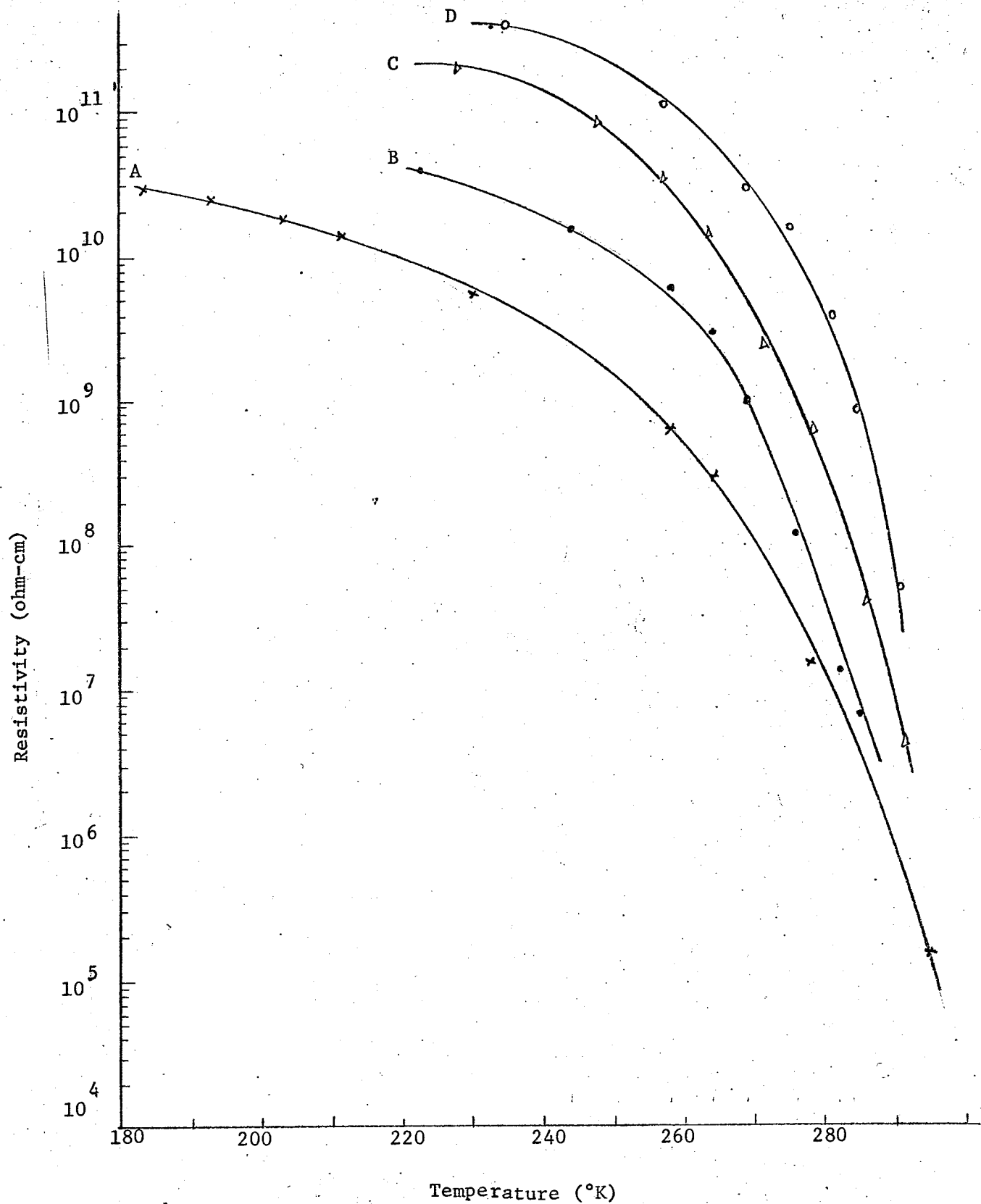


Fig. 4.9

The Temperature Dependence of Resistivity for a ZnSe Crystal before (crosses) and after (solid circles: 0.6×10^6 rads; triangles: 4.2×10^6 rads; circles: 9.2×10^6 rads.) Irradiation with ^{60}Co Gamma Rays. Applied Voltage = 400V. Magnetic Field = 0 Gauss

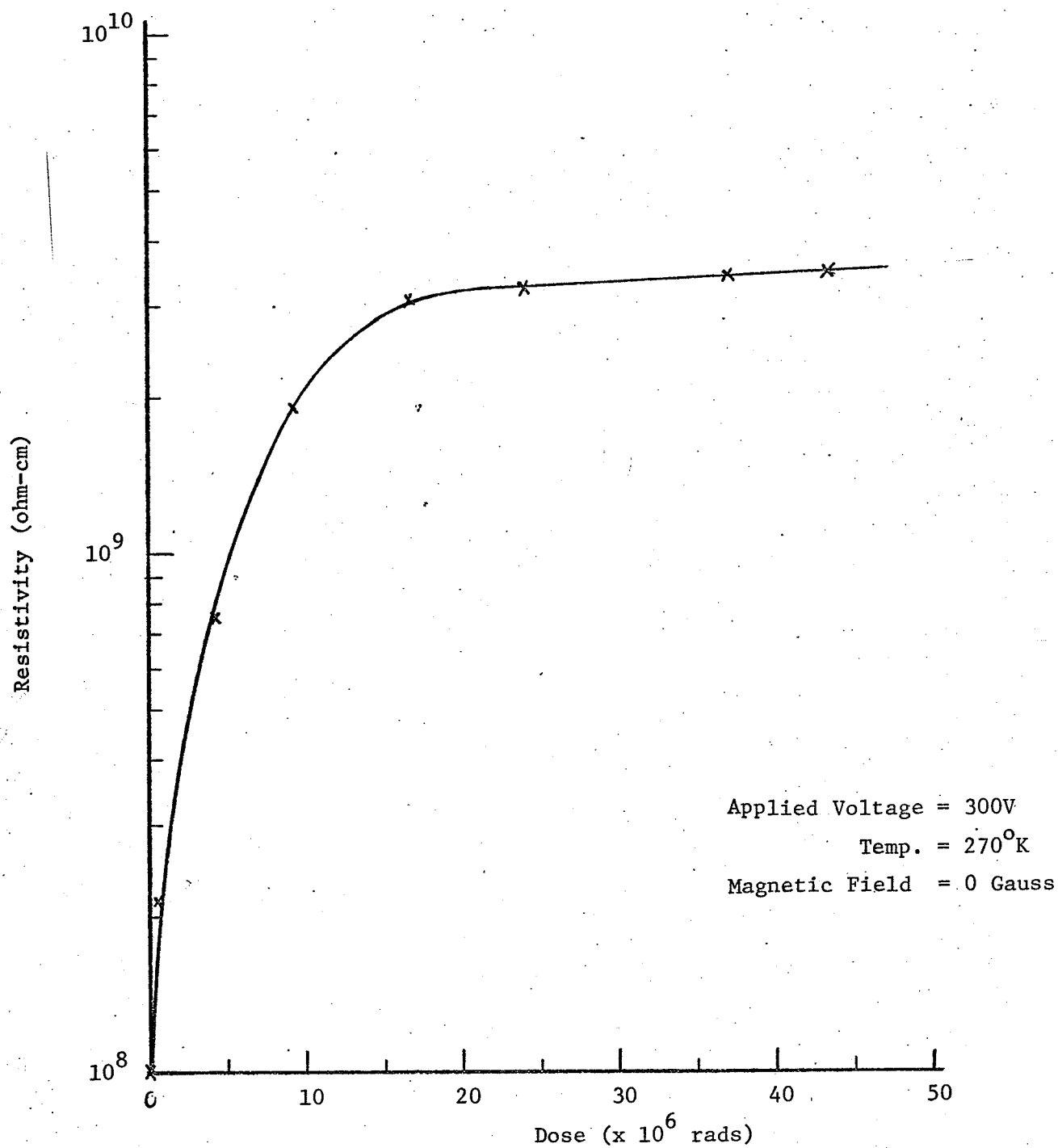


Fig. 4.10 Dependence of Resistivity of a ZnSe Crystal on Radiation Dose

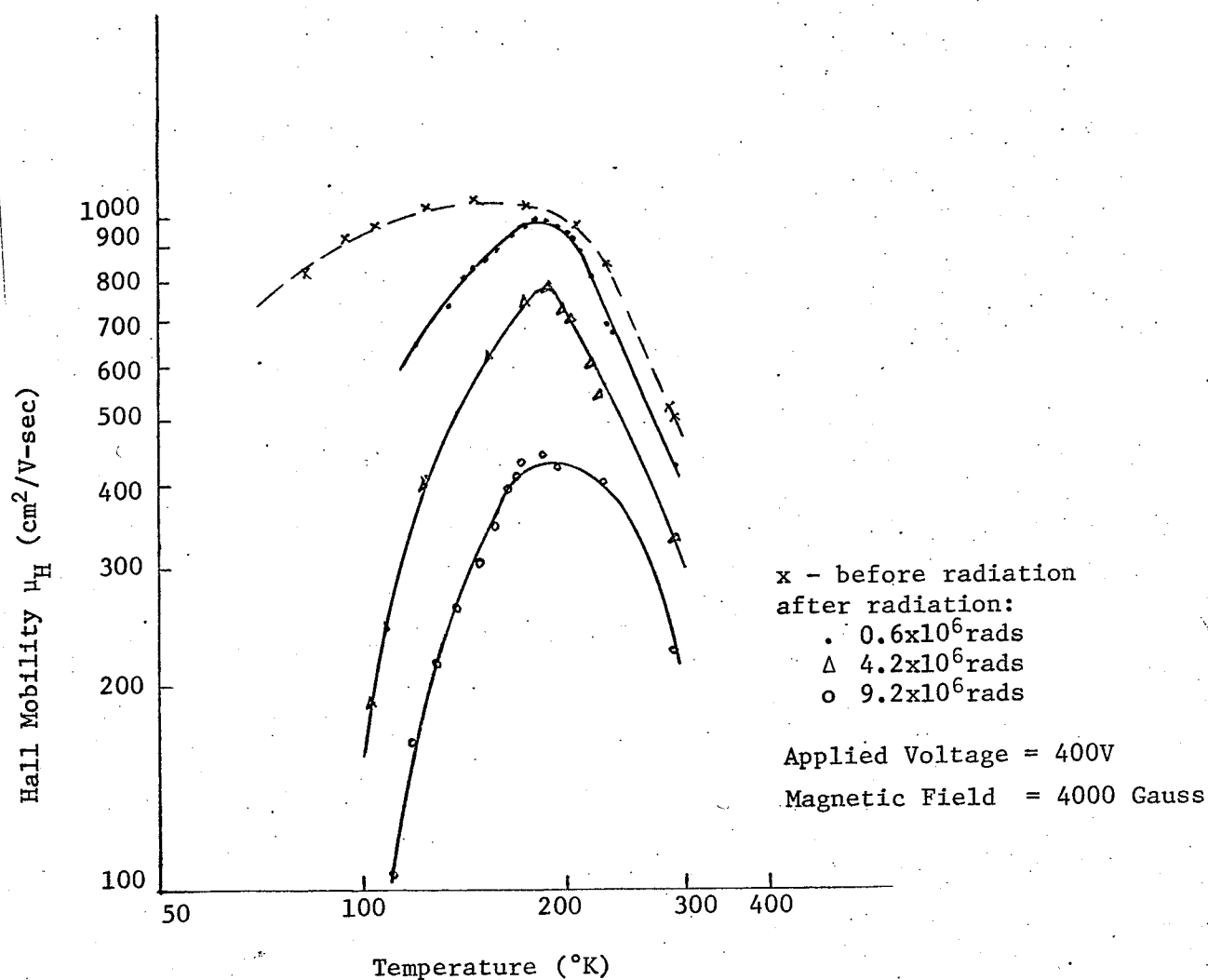


Fig. 4.11

The Temperature Dependence of Hall Mobility before and after Irradiation with ⁶⁰Co Gamma Rays

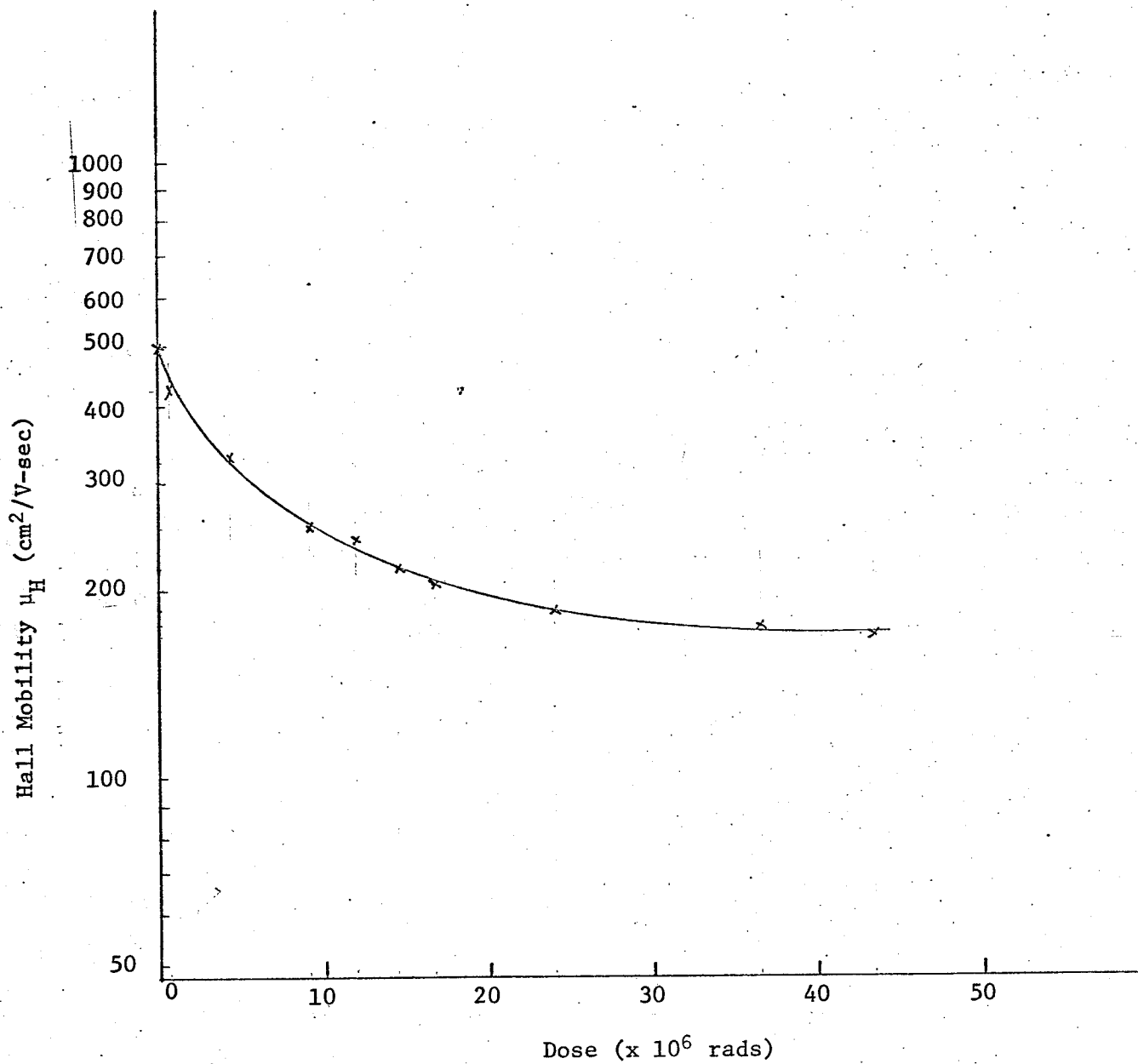


Fig. 4.12 The Effect of Gamma Irradiation on the Hall Mobility in ZnSe Crystal at room Temperature

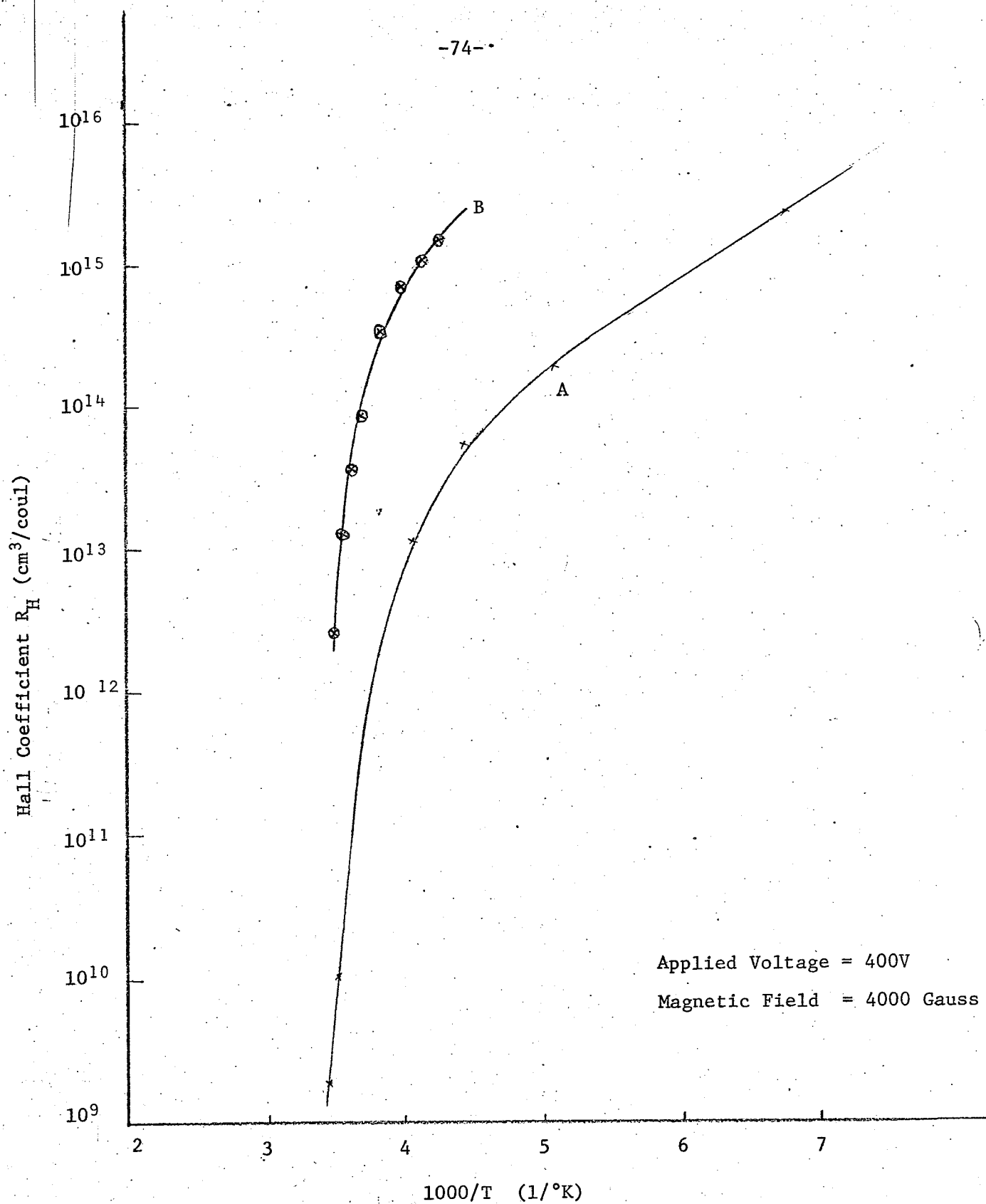


Fig. 4.13 The Temperature Dependence of Hall Coefficient before (Curve A) and after (Curve B: 9.2×10^6 rads.) Irradiation with ^{60}Co Gamma Rays

CHAPTER V

ANALYSIS AND DISCUSSION OF EXPERIMENTAL RESULTS

It has been shown by Billington and Crawford (1961) that in group IV and III-V semiconductors the ^{60}Co gamma radiation produces point defects which result in a shift of the Fermi level. Generally, a small amount of lattice damage introduced by gamma radiation in these semiconductors does not alter the lattice parameters, bonding strength, effective mass, or overall band structure. The effect of gamma radiation is due primarily to vacancies and interstitials which result in additional doping levels, trapping centres, and variation in carrier mobility. The effects of radiation upon the electrical properties of II-VI compounds have not yet been fully explored. Chester (1967) reported that in n-type CdS and n-type CdTe the radiation with ^{60}Co and ^{137}Cs gamma ray at room temperature did not introduce any new energy levels in the range from 0.02 to 0.2eV below the conduction band, although the density of levels initially present in this interval was altered and, under certain conditions, deep-lying acceptor states were produced.

Before discussing and analyzing the experimental results, it will be necessary to assume a value for the effective mass for the carrier. On the basis of previous work (see Table 2.2), we take $m^* = 0.17m$ as a reasonable estimate of the electron effective mass.

From the statistics for a multiple localized level and non-degenerate carrier densities, Blakemore (1962) showed that the number of ionized donors in i^{th} level may be written as

$$(N_{Di})_{\text{ion}} = \frac{N_{Di}}{1 + (n / \beta_i N_c) \exp(\frac{E_{Di}}{kT})} \quad (5.1)$$

where ' N_{Di} ' is the density of the i^{th} donor with a binding energy ' E_{Di} ' below the conduction band.

The sum of all ionized donors is equal to the conduction band electron density plus all electrons in compensating acceptors. Thus, the carrier concentration ' n ' is given by

$$n + N_A = \sum_{i=1}^M \frac{N_{Di}}{1 + (n / \beta_i N_c) \exp(\frac{E_{Di}}{kT})} \quad (5.2)$$

where ' M ' is the total number of donors, ' N_A ' is the total density of acceptors, ' β ' is the spin degeneracy of the i^{th} energy level, ' T ' is the absolute temperature, and

$$N_c = 2 \left(\frac{2\pi m^* kT}{h^2} \right)^{3/2} \quad (5.3)$$

where ' m^* ' is the effective mass of electrons, ' k ' is the Boltzmann's constant, and ' h ' is the Planck's constant. In the following, we take the carrier concentration ' n ' to be given by $r/|R_H q|$ where ' R_H ' is the Hall constant, ' q ' is the electronic charge and ' r ' is the ratio of Hall to drift mobilities ($r = \mu_H/\mu_D$) which is determined by the operative scattering mechanisms of the carriers, and for simplicity, ' r ' is taken to be unity. In fact, it is a fairly good approximation since ' r ' is reasonably close to unity for polar scattering which may be shown later to be the principal scattering mechanism in the temperature range of our primary interest. The experimentally measured parameters are ' R_H ', the Hall coefficient, and ' T ', the absolute temperature. Parameters ' N_{Di} ', ' E_{Di} ', and ' N_A ' were determined by the least-square analysis. The energy level spin degeneracy ' β_i ' which depends on the nature of the impurity state and the band edge involved, was set equal to unity. In general, ' β_i ' is unknown unless the detailed electronic structure of a centre is known.

In Eqn. (5.1), the donor levels are all assumed to be independent. This assumption is reasonable because there is no conclusively experimental evidence that associates closely spaced energy levels with a single donor centre. Also, it has been shown by Blakemore (1962) that multivalent donor or acceptor problems are not too different from those of independent donors present in identical amounts when the energy levels are well separated. In order to obtain information about the donor ionization

energy and the concentrations of donors and compensating acceptors, the carrier concentrations are analyzed on the basis of single level and non-degenerate conditions. From Eqn. (5.1), the carrier concentration 'n' can be written as

$$\frac{n(N_A + n)}{(N_D - N_A - n)} = \beta N_C \exp \left(- \frac{E_D}{kT} \right) \quad (5.4)$$

By fitting this expression to the experimental data with the computer aid, the values of N_A , N_D and E_D can be found. From Fig. 4.13, the carrier concentration can be calculated from the relation $n = 1/|R_H q|$. E_D can be estimated from the slope of $\ln(n)$ vs $1/T$ in the low temperature range. (Blakemore 1962). The method of least-squares can then be applied to Eqn. 5.3, to find the values of the parameters which give the best fit over the entire temperature range. The data are fitted satisfactorily using $N_D = 1.19 \times 10^{11} \text{cm}^{-3}$, $N_A = 3.94 \times 10^{10} \text{cm}^{-3}$ and $E_D = 0.316 \text{eV}$ for the condition before gamma radiation; and $N_D = 1.17 \times 10^9 \text{cm}^{-3}$, $N_A = 3.71 \times 10^8 \text{cm}^{-3}$ and $E_D = 0.377 \text{eV}$ after gamma radiation. These results indicate that a deep-lying acceptor level was produced by irradiation.

Qualitatively, support to the correlation suggested by gamma ray irradiation is given by charged particle bombardment data. If charged particles, such as electrons, protons, etc., bombard a binary semiconductor,

generally both types of atoms will be displaced. If the two types of atoms have the same displacement threshold and if the incident particle energy is a few MeV, then the atom with the largest atomic number will have the greatest displacement cross-section. The scattering law for charged particles favours low-energy transfer. In ZnSe, Kulp and Detweiler (1963) showed that at 240KeV an electron can transfer a maximum of 8.2eV to a selenium atom and 10eV to a zinc atom. As a result, electron bombardment should produce preferential Se displacement in ZnSe. Thus, it would be expected that charged particle bombardment of ZnSe would produce preferential acceptor introduction in ZnSe.

The introduction of acceptor type defects due to gamma ray irradiation is responsible for the increase of the resistivity of irradiated ZnSe. The Fermi level moves downward and the number of vacancies in the Se centre increases, which gives rise to the observed decrease in the effective lifetime (i.e. decrease in the Hall mobility) of the majority carriers. In ZnSe, the simplest acceptors will be Zn vacancies or Se atoms in interstitial sites. Since the threshold energy needed to displace the Se atoms to interstitial sites is smaller than the energy needed to displace Zn atoms, it is reasonable to assume that the selenide atoms will be displaced by the Compton electrons into interstitial sites more frequently than zinc atoms. Therefore, it is likely that the production of acceptor type defects by gamma rays in ZnSe is associated with interstitial Se atoms.

Before radiation, the Hall mobility ' μ_H ' increases with decreasing temperature, reaches a maximum at about 150°K and then decreases with decreasing temperature as shown in Fig. 4.11. It appears that as R_H increases rapidly with decreasing temperature for $T > 150^\circ\text{K}$ the mobilities are determined by the intrinsic properties of the materials rather than by the crystal defects. On the other hand, below about 150°K, charged impurity scattering becomes important as is indicated by the increase in mobility with temperature. It should be noted that a study of the mobility of ZnSe will, in general, parallel the corresponding studies of the more thoroughly investigated semiconductors in the III-V compound family. Ehrenreich (1961) suggested that at least for the n-type III-V compounds, the polar character plays a major role in their transport properties. This would also be expected to be true for the II-VI compounds because of their strongly polar nature.

In order to have a reasonably complete study for the intrinsic mobility of this material, four scattering mechanisms should be considered. These are scattering by the piezoelectric activity, the deformation potential, and the non-polar and polar interactions with the optical modes. For all these four scattering mechanisms, the mobility will drop off with increasing temperature. With a suitable $m^*(0.17m)$ this should provide us with results which are at least semiquantitatively correct. The mobility of carriers in a simple band with the interaction of the scattering by piezoelectrically active acoustic modes (Segall, Lorenz and Halsted, 1963)

is

$$\mu_{\text{piezo}} = 1.05 \rho \langle \mu_{\ell}^2 \rangle \epsilon_s^2 e_{14}^{-2} (m^*/m)^{-3/2} T^{-1/2} \text{cm}^2/\text{V-sec} \quad (5.5)$$

where ' ρ ' is the density, ' μ_{ℓ} ' is the longitudinal sound velocity, ' ϵ_s ' is the static dielectric constant, ' e_{14} ' is the piezoelectric constant (in esu/cm²) and ' m^* ' is the effective mass. The values of the various parameters used in Eqn. 5.5 are: $\epsilon_s = 8.1$, $e_{14} = 1.5 \times 10^4 \text{stat.coul/cm}^2$, $m^*/m = 0.17$, and $\rho \langle \mu_{\ell}^2 \rangle = 1.06 \times 10^{12} \text{dynes/cm}^2$. Then, the resulting mobility is

$$\mu_{\text{piezo}} \approx 2.67 \times 10^5 \left(\frac{300}{T} \right)^{1/2} \text{cm}^2/\text{V-sec} \quad (5.6)$$

This value well exceeds our measured Hall mobility (see Fig. 5.1). Thus, it indicates that this mechanism does not play an important role in determining the mobility for the ZnSe crystal.

The mobility for the scattering by the deformation potential can be expressed (Brooks, 1955) as

$$\mu_{\text{dp}} = 3.0 \times 10^{-5} (m^*/m)^{5/2} \rho \langle \mu_{\ell}^2 \rangle T^{-1/2} E_b^{-2} \text{cm}^2/\text{V-sec} \quad (5.7)$$

where ' E_b ' denotes the deformation potential for the relevant band edge.

Unfortunately, there is no direct information about these quantities for ZnSe. However, Aven and Segall (1963) suggested that there is a reasonable approximation by taking the value of 4eV as the deformation potential for the conduction band edge of ZnSe. With this value, the calculated mobility is

$$\mu_{dp} \approx 1.37 \times 10^3 \times \left(\frac{300}{T} \right)^{1/2} \text{ cm}^2/\text{V-sec} \quad (5.8)$$

Since this value is still much larger than our measured value, it appears that acoustic mode scattering is not important for ZnSe.

The scattering by the non-polar interaction with the optical phonons can be completely ruled out for n-type ZnSe for two reasons. First, the effective mass is small but the mobility scattered by this mechanism is proportional to $(m^*)^{-5/2}$. The second reason is that for the Γ_1 (s-like) conduction band minimum the matrix element for scattering between electronic states \bar{k} and \bar{k}' vanishes to lowest order in the phonon wave vector $\bar{q} = \bar{k} - \bar{k}'$. The reduction in the scattering due to this selection rule is $\sim 10^{-3}$.

The last and most important mechanism to be considered is the scattering of the carriers by the electric polarization associated with the optical modes. The strength of the interaction depends on the polar coupling constant α (Segall, Lorenz and Halsted, 1963) which is

$$\alpha = (m^*/m)^{1/2} (Ry/\hbar\omega_l)^{1/2} (\epsilon_\infty^{-1} - \epsilon_s^{-1}) \quad (5.9)$$

where 'Ry' is the Rydberg of energy, $\hbar\omega_l$ (~0.0314eV for ZnSe) is the energy of the longitudinal optical mode for long wavelength, and ϵ_∞ (~5.75) is the high frequency or optical dielectric constant. Using the relevant parameters, given above, we find that $\alpha \approx 0.46$ for electrons in ZnSe. Then, the mobility due to this scattering mechanism can be written (Segall, Lorenz and Halsted, 1963) as

$$\mu_{\text{polar}} = \frac{0.870(m/m^*)}{\alpha\hbar\omega_l} \left[\frac{e^z - 1}{z^{1/2}} \right] G(z) e^{-\xi} \quad (5.10)$$

where $z = \hbar\omega_l/kT$, $\hbar\omega_l$ is in eV, and $G(z) e^{-\xi}$ is a tabulated function which has been evaluated by Horwarth and Sondheimer (1953) and generalized by Ehrenreich (1959). The value obtained from Eqn. 5.10 is shown in Fig. 5.1. In contrast to the other mechanisms considered, polar scattering leads to results which are very close to the experimental ones. The difference between these may be due to the temperature dependence of the relevant parameters such as ϵ_s , ϵ_∞ and $\hbar\omega_l$. The polar optical mode scattering clearly dominates the intrinsic scattering of electrons in ZnSe, the scattering from all other mechanisms such as the piezoelectric activity of the acoustic modes, the deformation potential, and the non-polar interaction with the optical modes being less important.

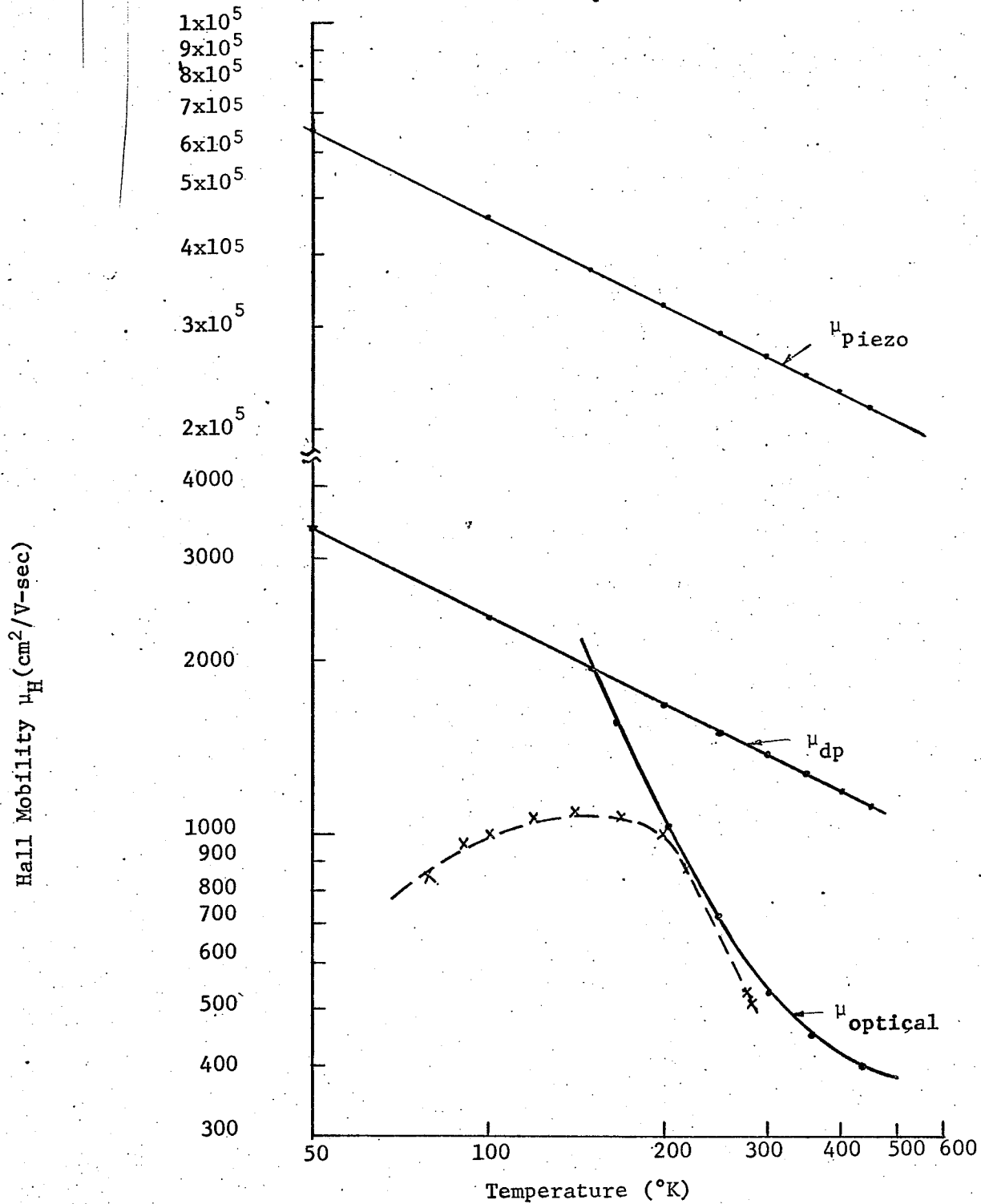


Fig. 5.1

Comparison of the Experimental Results of the Hall mobility before Gamma Irradiation with Theory for the Polar Optical Scattering (μ_{optical}), the deformation potential scattering (μ_{dp}), and the piezoelectrical mode scattering (μ_{piezo})

CHAPTER VI

CONCLUSION

In ZnSe, the simplest acceptors will be Zn vacancies or Se atoms in interstitial sites. It is well known that the threshold energy which an electron must have to displace the Se atoms to interstitial sites is smaller than the energy needed to displace Zn atoms. Therefore, if we take into account the possibility of multiple production of defects by a single Compton electron, it is reasonable to assume that the Selenide atoms will be displaced by the electrons into interstitial sites more frequently than Zinc atoms. Since the decrease in the dark resistivity and the concentration of majority carriers, it can be concluded that gamma irradiation produces acceptor type defects in ZnSe single crystal and that these acceptor type defects are associated with interstitial Se atoms.

The Hall mobility data in the present study strongly suggest that the mobility for $T \gtrsim 150^\circ\text{K}$ is determined by the intrinsic properties of the crystal. Simple analyses indicates that polar optical mode scattering clearly dominates over the scatterings by the piezoelectric activity of the acoustic modes, by the deformation potential, and by the non-polar interaction with the optical modes. The decrease in mobility over the whole range of temperatures is a good indication that a large number of scattering centres were introduced into the single crystal by gamma irradiation.

Further studies on the effects of gamma radiation on the optical properties of ZnSe, the radiation damage on the electronic properties at lower temperatures and at different irradiation temperatures, will be required in order to obtain a better understanding of the effects of gamma radiation in ZnSe crystal.

BIBLIOGRAPHY

A. BOOKS

- Aven, M. and J.S. Prener (ed.), Physics and Chemistry of II-VI Compounds, New York, Wiley, 1967
- Bethe, H.A. and J. Ashkin, Experimental Nuclear Physics, E. Segre (ed.), New York, Wiley, 1953
- Billington, D.S. and J.H. Crawford Jr., Radiation Damage in Solids, Princeton University Press, 1961
- Blakemore, J.S., Semiconductor Statistics, New York, Pergamon Press, 1962
- Chadderton, L.T., Radiation Damage in Crystals, New York, Wiley, 1965
- Gunnarsen, E.M. and G. George, Radiation Damage in Semiconductors, Paris, Dunod Cie, 1965
- Kircher, J.F. and R.E. Bowman (ed.), Effect of Radiation on Materials and Components, New York, Reinhold, 1964
- Putley, E.H., The Hall Effect and Related Phenomena, London, Butterworths, 1960
- Smith, R.A., Semiconductors, Cambridge University Press, 1961
- Vavilov, V.S., Effects of Radiation on Semiconductors, New York, Consultants Bureau, 1965

B. PERIODICALS

- Ankerman, L.W., Radiation Produced Energy Levels in Compound Semiconductors, J. Appl. Phys., Vol. 30, No. 8, p. 1239, Aug. 1959

- Aven, M. and P.R. Kennicott, Semiconductor Device Concepts, Scientific Report No. 8, Contract No. AF-19 (628) - 329, U.S. Air Force Cambridge Research Laboratories, Bedford, Massachusetts, p. 17, 1964
- Aven, M., D.T.F. Marple, and B. Segall, Some Electrical and Optical Properties of ZnSe, J. Appl. Phys., Suppl. to Vol. 32, No. 10, pp. 2261-2265, Oct. 1961
- Aven, M. and B. Segall, Carrier Mobility and Shallow Impurity States in ZnSe and ZnTe, Phys. Rev., Vol. 130, No. 1, pp. 81-91, Apr. 1963
- Blatt, F., Theory of Mobility of Electrons in Solids, Solid State Physics, Vol. 4, p. 200, 1957
- Brooks, H., Advan. Electron. Electron Phys., Vol. 7, p. 156, 1955
- Chester, R.O., Radiation Damage in Cadmium Sulfide and Cadmium Telluride, J. Appl. Phys., Vol. 38, No. 4, pp. 1745-1751, March 1967
- Collins, R.J., Mechanism and Defect Responsible for Edge Emission in CdS, J. Appl. Phys., Vol. 30, pp. 1135-1140, Aug. 1959
- de Nobel, D., Phase Equilibria and Semiconducting Properties of Cadmium Telluride, Philips Res., Repts. 14, pp. 361-399, and pp. 430-492, 1959
- Detweiler, R.M. and B.A. Kulp, Annealing of Radiation Damage in ZnSe, Phys. Rev., Vol. 146, No. 2, pp. 512-516, June 1966
- Devlin, S.S., Appendix to L.R. Shiozawa and J.M. Jost, 1965, Research on II-VI Compound Semiconductors, Final Technical Report

Contract No. AF 33(657)7399, U.S. Air Force Aeronautical
Research Laboratories, Wright Patterson Air Force Base, Ohio

Devlin, S.S., Physics and Chemistry of II-VI Compounds, New York, Wiley,
p. 566, 1967

Ehrenreich, H., J. Phys. Chem. Solids 8, p. 130, 1959

Ehrenreich, H., Band Structure and Electron Transport of GaAs, Phys. Rev.,
Vol. 120, No. 6, pp. 1851-1963, Dec. 1960

Ehrenreich, H., Band Structure and Transport Properties of Some III-V
Compounds, J. Appl. Phys., Suppl. to Vol. 32, No. 10, pp. 2155-
2166, Oct. 1961

Frohlich, H., Electrons in Lattice Fields, Advan. Phys., Vol. 3, pp. 325-
361, 1954

Galushka, A.P., I.B. Frmolovich, N.E. Korsunskaya, I.D. Konozenka, and
M.K. Sheinkman, Effect of Gamma and Fast Neutron Radiation on
the Electrical Properties of Cadmium Sulfide Single Crystals,
Sov. Phys., Solid State, Vol. 8, No. 8, pp. 831-837, Oct. 1966

Ho, B.I. and R.H. Bube, Photoelectronic Evaluation of Electron Radiation
Damage in CdS Crystals, J. Appl. Phys., Vol. 39, No. 6,
pp. 2908-2914, May 1968

Howarth, D.J. and E.H. Sondheimer, Proc. Roy. Soc. (London), A219,53 (1953)

Ikama, H., O. Datmurua and H. Suzuki, Gamma Ray Induced Conductivity of
CdS, J. Appl. Phys., Japan, Vol. 1, No. 4, pp. 236-7, Oct.
1962

Itakma, M. and H. Toyoda, Electrical Conductivity and Hall Coefficient of CdS Single Crystal, J. Phys., Soc. Japan, Vol. 18, No. 1, pp. 150-1, Jan. 1963

Johnson, R.T., Fast Neutron Irradiation Effects in CdS, J. Appl. Phys., Vol. 39, No. 8, pp. 3517-3526, July 1968

James and Harozikz

Kulp, B.A., Displacement of the Cadmium Atom in Single Crystal CdS by Electron Bombardment, Phys. Rev., Vol. 125, No. 6, pp. 1865-1869, March 1962

Kulp, B.A., Fluorescence Studies on II-VI Compound Semiconductors, 7th International Conference on the Physics of Semiconductors, Vol. 3, New York, Academic Press, p. 173, 1964

Kulp, B.A. and R.W. Detweiler, Threshold for Electron Radiation Damage in ZnSe, Phys. Rev., Vol. 129, No. 6, pp. 2422-2424, March, 1963

Kulp, B.A. and R.W. Detweiler, Electron Radiation Damage in ZnSe at Low Temperature, 7th International Conference on the Physics of Semiconductors, Vol. 3, pp. 385-392, 1964

Kulp, B.A. and R.H. Kelly, Displacement of the Sulfide Atom in CdS by Electron Bombardment, J. Appl. Phys., Vol. 31, p. 1057, 1960

Kurik, M.V., Electron Effective Mass in II-VI Semiconductors, Phys. Letters, Vol. 24, No. 13, Jan. 1967

Lorenz, M.R., M. Aven and H.H. Woodbury, Correlation Between Irradiation and Thermally Induced Defects in II-VI Compounds, phys. Rev., Vol. 132, No. 1, p. 143, Oct. 1963

- Lorenz, M.R. and B. Segall, Shallow and Deep Acceptor States in CdTe,
Phys. Letter, Vol. 7, No. 1, pp. 18-20, Oct. 1963
- Lorenz, M.R. and B. Segall, and H.H. Woodbury, Some Properties of a Double
Acceptor Centre in CdTe, Phys. Rev., Vol. 134, No. 3A, p. A751,
May 1964
- Lorenz, M.R. and H.H. Woodbury, Double Acceptor Defects in CdTe, Phys.
Rev. Letter, Vol. 10, No. 6, pp. 215-217, March 1963
- Marple, D.T.F., Electron Effective Mass in ZnSe, J. Appl. Phys., Vol. 35,
No. 6, pp. 1879-1882, June 1964
- Masumi, T., Relaxation Time Anisotropy in Cadmium Sulfide Studied with
Electrical Resistivity and Magnetoresistance Effect, J. Phys.
Soc. Japan, Vol. 14, No. 1, pp. 47-56, Jan. 1959
- Oswald, Jr. R.B. and C. Kikuchi, Nucl. Sci. Eng., Vol. 23, p. 354, 1965
- Reynolds, D.C., Edge Emission in Zinc Selenide Single Crystals, J. Appl.
Phys., Suppl. to Vol. 32, No. 10, p. 2250, Oct. 1961
- Reynolds, D.C., L.C. Greene, S.J. Czyzak and W.M. Baker, Method for Growing
Large CdS and ZnS Single Crystals, J. Chem. Phys., Vol. 29,
No. 6, pp. 1375-1380, Dec. 1958
- Riccius, H.D. and R. Turner, Determination of the Reduced Effective Mass
in Zinc Selenide, J. Phys. Chem. Solids, Vol. 28, pp. 1623-1624,
1967
- Schulze, R.G. and B.A. Kulp, On the Conductivity of CdS Following Electron
Bombardment, J. Appl. Phys., Vol. 33, No. 7, pp. 2173-2175, July
1962

Schulze, R.G. and B.A. Kulp, Electron Radiation Damage in Cadmium Selenide Crystals at Liquid Helium Temperatures, Phys. Rev., Vol. 159, No. 3, July 1967

Spear, W.E. and J. Mort, Electron and Hole Transport in CdS Crystals, Proc. Phys. Soc. London, Vol. 81, pp. 130-140, July 1963

Wheeler, R.G. and J.O. Dimmock, Exciton Structure and Zeeman Effects in Cadmium Selenide, Phys. Rev., Vol. 125, No. 6, p. 1805, March 1962

Woodbury, H.H. and M. Aven, Some Electrical Transport Studies on n-type II-VI Semiconductors, 7th International Conference on the Physics of Semiconductors, Vol. 3, New York, Academic Press, p. 179, 1965

Zook, D., Piezoelectric Scattering in Semiconductors, Phys. Rev., Vol. 136, No. 3A, pp. A869-A878, Nov. 1964

Zook, D. and R.N. Dexter, Galvanomagnetic Effects in Cadmium Sulfide, Phys. Rev., Vol. 129, No. 5, pp. 1989-1990, March 1963